Meteoritics 29, 182–199 (1994)

The Divnoe meteorite: Petrology, chemistry, oxygen isotopes and origin

M. I. PETAEV[1,2], L. D. BARSUKOVA[2], M. E. LIPSCHUTZ[3], M.-S. WANG[3], A. A. ARISKIN[2], R. N. CLAYTON[4,5] and T. K. MAYEDA[5]

[1]Harvard-Smithsonian Center for Astrophysics, Cambridge, Massachusetts 02138, USA
[2]Vernadsky Institute of Geochemistry and Analytical Chemistry, Russian Academy of Sciences, Moscow 117195, Russia
[3]Department of Chemistry, Purdue University, West Lafayette, Indiana 47907, USA
[4]Department of Chemistry, University of Chicago, Chicago, Illinois 60637, USA
[5]Enrico Fermi Institute, University of Chicago, Chicago, Illinois 60637, USA

(Received 1993 May 14; accepted in revised form 1993 November 29)

Abstract—The Divnoe meteorite is an olivine-rich primitive achondrite with subchondritic chemistry and mineralogy. It has a granoblastic, coarse-grained, olivine groundmass (CGL: coarse-grained lithology) with relatively large pyroxene-plagioclase poikilitic patches (PP) and small fine-grained domains of an opaque-rich lithology (ORL). Both PP and ORL are inhomogeneously distributed and display reaction boundaries with the groundmass. Major silicates, olivine (Fa_{20-28}) and orthopyroxene ($Fs_{20-28}Wo_{0.5-2.5}$), display systematic differences in composition between CGL and ORL as well as a complicated pattern of variations within CGL. Accessory plagioclase has low K content and displays regular igneous zoning with core compositions An_{40-45} and rims An_{32-37}. The bulk chemical composition of Divnoe is similar to that of olivine-rich primitive achondrites, except for a depletion of incompatible elements and minor enrichment of refractory siderophiles. Oxygen isotope compositions for whole-rock and separated minerals from Divnoe fall in a narrow range, with mean $\delta^{18}O = +4.91$, $\delta^{17}O = +2.24$, and $\Delta^{17}O = -0.26 \pm 0.11$. The isotopic composition is not within the range of any previously recognized group but is very close to that of the brachinites. To understand the origin of Divnoe lithologies, partial melting and crystallization were modelled using starting compositions equal to that of Divnoe and some chondritic meteorites. It was found that the Divnoe composition could be derived from a chondritic source region by ~20 wt% partial melting at T ≈ 1300 °C and $\log(fO_2) = IW-1.8$, followed by ~60 wt% crystallization of the partial melt formed, and removal of the still-liquid portion of the partial melt. Removal of the last partial melt resulted in depletion of the Divnoe plagioclase in Na and K. In this scenario, CGL represents the residue of partial melting, and PP is a portion of the partial melt that crystallized *in situ*. The ORL was formed during the final stages of partial melting by reaction between gaseous sulfur and residual olivine in the source region.

A prominent feature of Divnoe is fine μm-scale chemical variations within olivine grains, related to lamellar structures the olivines display. The origin of these structures is not known.

INTRODUCTION

The Divnoe meteorite was found in 1981 in Stavropol province, Russia (Graham, 1983). It is 30 x 18 x 11 cm in dimension, weighs 12.7 kg, and is covered by fusion crust that is rusty brown as a result of terrestrial weathering. A morphological study of the meteorite was made by Krinov (1984), who concluded it is one of a shower that fell; however, no other specimens of Divnoe have been found to date.

Previous studies (Zaslavskaya *et al.*, 1990; Zaslavskaya and Petaev, 1990; Petaev *et al.*, 1990b,c; Petaev and Zaslavskaya, 1990; Smoliar *et al.*, 1991; Petaev and Ariskin, 1992) reported the meteorite to be a rather heterogeneous, olivine-rich achondrite with high contents of troilite and metal. These authors noted that it is depleted in incompatible elements, and it has experienced a relatively severe shock event (Zaslavskaya and Petaev, 1990). Chemical and mineralogical studies of the meteorite suggest that it resulted from early partial melting of subchondritic precursor material, followed by *in situ* crystallization of about 50% of the partial melt (Petaev and Ariskin, 1992); following this, the residual melt, enriched in incompatible elements, was removed. Later the meteorite experienced intense subsolidus recrystallization (~700 Ma ago?; Smoliar *et al.*, 1991). It was ejected from its parent body and exposed to cosmic radiation at least 20 Ma ago (Petaev *et al.*, 1990c). Mineralogical, chemical, and isotopic studies (Petaev and Zaslavskaya, 1990) have revealed no direct relationship with any known meteorite type, but Divnoe is structurally and chemically similar to other primitive achondrites.

Zaslavskaya *et al.* (1990) noted that Divnoe is coarse-grained and inhomogeneous, and that a detailed study was needed of larger and more representative samples than the one they reported on. Herein we present the results of such a study.

SAMPLES STUDIED AND TECHNIQUES

New polished slabs of ~25 cm^2 and ~2.7 cm^2 area and older polished slabs and thin sections having ~6 cm^2 total area were studied by optical microscopy and EPMA, using a JEOL 733 imaging electron microprobe with wavelength dispersive spectrometers for point analyses and X-ray element distribution maps. Analyses were performed using accelerating voltages of 15 kV for silicates and 20 kV for metal and troilite, and 20 nA beam current (measured with a Faraday cup). The standards used were meteoritic olivine (for SiO_2, MgO, FeO), synthetic Al-enstatite (Al_2O_3), Ni-diopside (NiO), a silicate glass (MnO), natural plagioclase (CaO, Na_2O), K-feldspar (K_2O), hornblende (TiO_2), chromite (Cr_2O_3), apatite (P_2O_5), pyrite (S), and metallic Fe, Ni, Co, Cu, and Si. The data were reduced using standard Bence-Albee and ZAF correction procedures. Counting errors (1σ) associated with analyses of olivine and pyroxene were 0.1 mol% Fa, 0.1% Fo, 0.2% Fs, 0.2% En, and 0.1% Wo. Modal compositions of selected section areas and the proportions of low- and high-Ca pyroxenes in exsolved pyroxene grains were calculated by point counting on BSE images.

To avoid sampling problems in isotopic and bulk chemical studies, we homogenized a large specimen of the meteorite (12.26 g; 2.0 x 1.5 x 1.5 cm). The specimen was crushed in a steel mortar, after which most of the material was powdered in a jasper mortar. The magnetic fraction (8.62 wt%) was removed from this powder using a hand magnet. The subsample intended for the determination of alkalies, C, S, and H_2O was powdered without alcohol. Aliquots of the bulk sample, non-magnetic,and magnetic fractions were distributed among the laboratories involved in this study.

Wet chemical analysis was performed using traditional techniques (D'yakonova *et al.*, 1979). Major elements were determined by X-ray fluorescence, atomic absorption, and ICP methods; H_2O and C contents were measured with a CHN-analyzer. Ferrous iron was calculated based on the amounts of the acid-soluble ($3HCl + HNO_3$) and insoluble fractions (53.43 and 46.57 wt%, respectively).

Two samples of Divnoe were analyzed by RNAA: a 115-mg aliquot of a non-magnetic separate prepared at the Vernadsky Institute, and a 177-mg whole rock chip. These samples were sealed in quartz irradiation vials of the type in standard use at Purdue University and were irradiated with other samples and monitors, at the University of Missouri Research Reactor at a flux of 8 x 10^{13} $n/cm^2/sec$ for 20 days (non-magnetic separate) or 10 days (whole rock-chip). Monitor preparation, chemical processing, counting procedures, and data reduction techniques were similar to those described by Wolf (1993). Chemical yields were satisfactory, exceeding 50% for all elements but Ag (29%), Cs (43%), and Sb (46%) for the non-magnetic separate; and Ag (30%), In (38%), Cs (40%), and Au (43%) for the whole-rock sample. Chemical yields for monitors exceeded 50% for all elements and ranged up to 99%.

Oxygen isotope compositions were measured of an aliquot of the non-magnetic fraction: integral chips (enriched in olivine and pyroxene respectively;) two hand-picked mineral separates, and coarse- and fine-grained crushed material left after mineral separation. One of the hand-picked mineral separates consisted of clear transparent grains having a refractive index similar to that of pyroxene, and the other consisted of dark, nontransparent intergrowths

of a silicate with opaque minerals, mainly troilite. The silicate in this second separate was tentatively identified as olivine rather than pyroxene, but this identification has not been confirmed. The mineralogy of the coarse- and fine-grained crushed material is expected to be close to the bulk Divnoe mineralogy; the fine-grained fraction may be slightly enriched in pyroxenes.

PETROGRAPHY

In the hand specimen, the Divnoe meteorite is seen to be a dark, almost black, crystalline rock with inhomogeneously distributed metal and troilite grains. At one of the cut surfaces, a preferred alignment of metal grains and veins can be seen, suggestive of the possible role of either stress or viscous flow in formation of the meteorite. Many thin sections of the customary size display clear granoblastic texture (Fig. 1); the grain size is coarse but variable (up to ~2 mm), and the sections are saturated with thin veinlets of opaque minerals which are located at grain boundaries and fill pre-existing cracks. One thin section displays pronounced preferable alignment of all mineral grains.

The coarse-grained host rock contains numerous finer-grained, opaque-mineral-rich domains, which tend to be translucent or even opaque by transmitted light (Fig. 1). In previous studies of the meteorite, these domains were referred to as "fine-grained" (Zaslavskaya *et al.*, 1990) or "dark lithology" (Zaslavskaya and Petaev, 1990), but we show below that their most important property is enrichment in opaque minerals. This enrichment has genetic significance, so we will stress the mineralogy by calling these domains "opaque-rich lithology" (ORL). The granoblastic groundmass enclosing ORL will be referred to as "coarse-grained lithology" (CGL).

The CGL also contains large (mm to cm), inhomogeneously distributed anhedral poikilitic patches (PP) of pyroxene (Fig. 2) and (rarely) plagioclase (Fig. 3). The greatest amount of PP (Table 1) was found in the large slab studied, where the patches show preferred orientation parallel to elongated metal grains, large cracks, and veins formed by cracks filled with opaque minerals.

Another textural constituent of Divnoe consists of large metal-sulfide veins, which often contain inclusions of silicates and

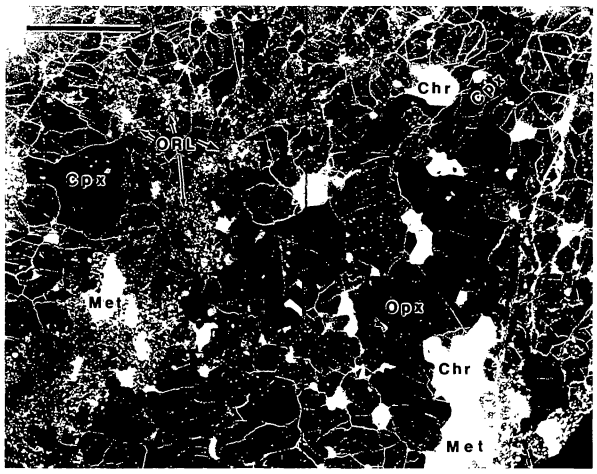

FIG. 2. Textural relationships among Divnoe lithologies (BSE image photomosaic). Scale bar, 1 mm. Gray, olivine; white, opaque minerals; dark gray, pyroxenes. Opx, low-Ca pyroxene; Cpx, high-Ca pyroxene; Chr, chromite; Met, metal. ORL, opaque-rich lithology. The CGL olivine grains as well as poikilitic olivines are more rounded at boundaries between CGL and PP than they are within CGL. The PPs consist of large anhedral pyroxene grains containing poikilitic inclusions of rounded olivines and clusters of metal and chromite (right bottom). A long branching ORL vein (left) crosses olivine and metal grains in CGL and displays reactionary contacts with them. Olivine and pyroxene contain numerous opaque veins and tiny inclusions of metal and troilite.

chromite, and intergrowths of these minerals with one other as well as with ORL. Sometimes veins cross PP and displace fragments of poikilitic grains. This implies they were formed after the major meteorite lithologies.

Coarse-grained Lithology

The coarse-grained lithology (CGL) consists mainly of olivine (0.3–1 mm across) with a small number of large (up to 1–2 mm) grains of metal and chromite (Figs. 1, 2). Most of the grains have almost straight boundaries, which usually meet one other at triple junction angles of ~120°. Individual troilite grains up to several

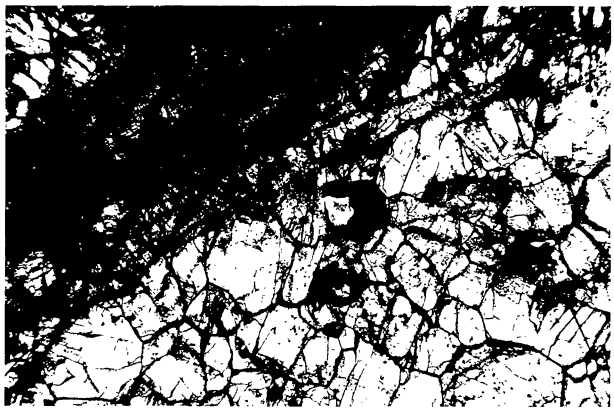

FIG. 1. Textures of coarse-grained (CGL, right bottom) and opaque-rich (ORL, broad black strip at the upper left corner) lithologies in Divnoe (transmitted light; width of field 3.1 mm). Large olivine grains in CGL often meet each other at triple junction angles of ~120°. Many olivines have irregular or planar fractures, often filled by opaque minerals (black). The grains themselves are separated from each other by opaque films (black) of varying thickness. The ORL consists of a much finer-grained intergrowth of pyroxene, olivine, and opaque minerals and is non-transparent because of the high content of the latter. Some of the larger transparent grains are olivine in reaction relationship with ORL.

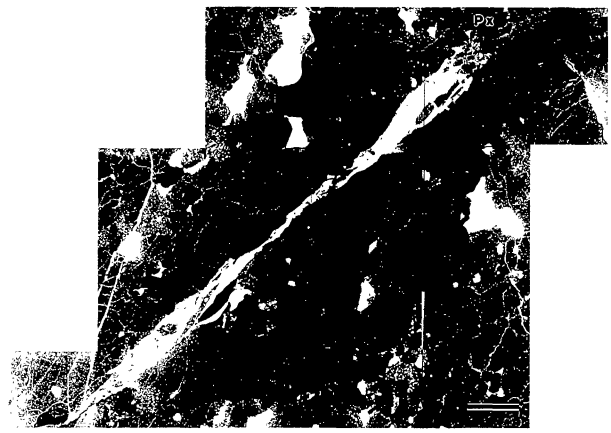

FIG. 3. A plagioclase-rich portion of the large section. BSE image photomosaic; scale bar, 1 mm. Black areas, plagioclase; black lines, open cracks; medium gray, pyroxene (Px); light gray groundmass, olivine; white, opaque minerals. Anhedral plagioclase fills spaces between olivine grains. A relatively thick metal-troilite vein, crossing all lithologies, contains fragments of silicates and shows no reaction with the groundmass. Rare ORL domains are located only within CGL and show no relation to the large vein.

hundreds of μm occur between other minerals. Metal and troilite in contact is rare within CGL.

Olivine and, sometimes, chromite contain numerous inclusions of troilite and/or metal. Most of these have droplet-like or irregular shapes, but some euhedral troilite grains also have been found. Some olivine grains contain areas enriched in inclusions of this type. Chromite and, rarely, metal contain olivine inclusions. Rare anhedral whitlockite grains, up to several hundred microns in size, are associated with large metal grains. Olivine, metal, and troilite grains in contact with ORL (Fig. 2) tend to be more or less irregular in shape, while the same grains retain their straight or slightly curved outlines at boundaries with CGL minerals. Most olivine grains have undulatory extinction and some display mosaicism, though this is not as pronounced as in heavily shocked meteorites. Among the numerous irregular fractures (usually filled by opaque mineral), some planar fractures are also observed.

In back-scattered electron images (BSE), many, if not all, olivine grains show a striated (Fig. 4) or spotty appearance, which seems to be crystallographically controlled. This μm-scale structure resembles exsolution lamellae and is accompanied by minor chemical variations. The structure of these grains looks similar to that of ringwoodite [γ-$(Mg,Fe)_2SiO_4$] and wadsleyite [β-$(Mg,Fe)_2SiO_4$] from shock-melted veins of ordinary chondrites (Price *et al.*, 1979, 1982; Price, 1983; Madon and Poirier, 1983) and olivine polymorphs produced by static high-pressure experiments (*e.g.*, Brearley *et al.*, 1992). Major differences between Divnoe olivines and the high-pressure olivine polymorphs listed are the scale of the structure (about two orders of magnitude greater in Divnoe), and the presence of only the anisotropic α-polymorph of olivine in Divnoe.

Among several lamellar olivine grains studied by both BSE imaging and transmitted light, one was found to display 5–12 μm-thick lamellae with the same orientation and thickness as the lamellae seen in back-scattered electron images (Fig. 5). The structure of the grain looks similar to that of terrestrial lamellar olivine (Deer *et al.*, 1982), but the latter does not show chemical differences between lamellae.

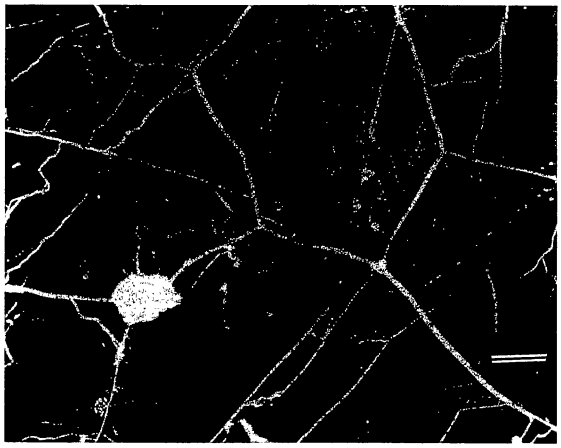

FIG. 4. Lamellar structure in olivine grains. BSE image; scale bar, 50 μm. Gray, olivine; different tones signify compositional differences. White, opaque minerals (mainly troilite and Fe oxides). Differences in the lamellae orientation between olivine grains indicate the lamellae are crystallographically controlled.

Opaque-rich Lithology

Opaque-rich lithology has been found only within CGL and is often at boundaries between olivine grains, or along pre-existing cracks now filled by ORL. The modes of occurrence of ORL (Figs. 1, 2) vary from roughly equidimensional, irregular areas ranging in size from tens to hundreds of μm, to long (several mm) branching veins of variable thickness (100–900 μm). Sometimes ORL is associated with large metal or troilite grains. The texture of ORL depends upon its content of opaque minerals, changing from xenoblastic to micrographic as the content of opaques and the troilite/metal ratio increases. The grain size of ORL rarely exceeds 100 μm, and varies (from one ORL area to another) from several μm to tens of μm, being relatively constant within each area.

The major minerals (Table 1) are low-Ca pyroxene (or, rarely, two pyroxenes with slightly different compositions ($Fs_{22.2}Wo_{1.0}$ and

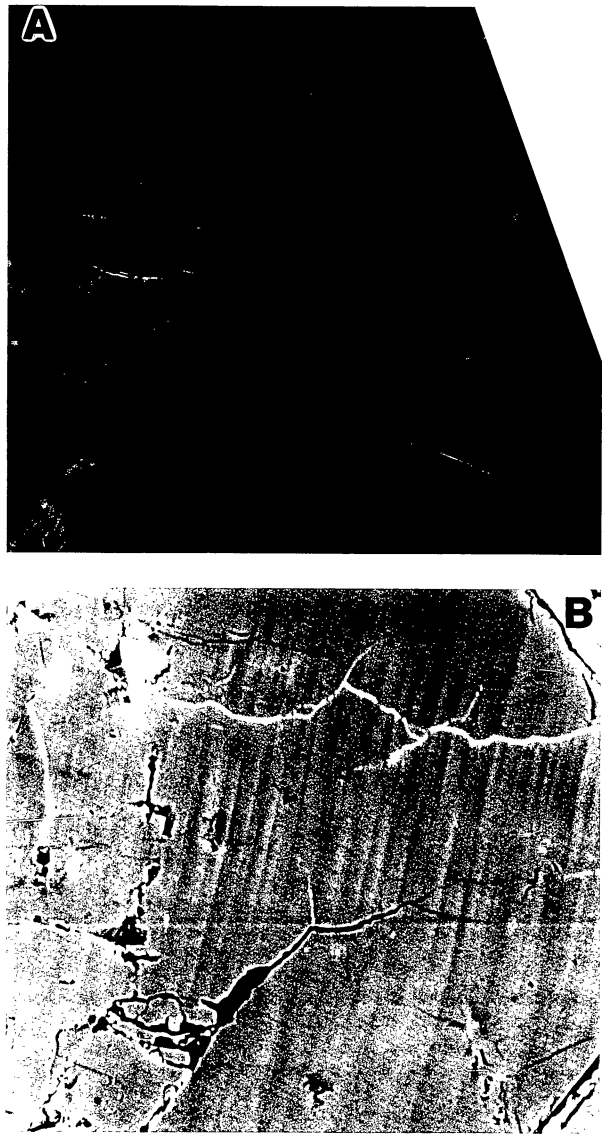

FIG. 5. Lamellar structure in olivine. Width of field, 190 μm. (a) Transmitted light, crossed nicols; rounded spot at the bottom is a section defect. (b) BSE image. Note the correspondence of orientations and thicknesses of lamellae in the two images.

TABLE 1. Mineralogy of Divnoe lithologies (vol.%)

	Bulk[1]	PP-rich	ORL
Olivine	74.6	57.9	32
Pyroxene	14.3	27.6	41
Plagioclase	1.5	n.d.	n.d.
PP	(15.8)[2]	(27.6)[2]	n.d.
ORL	-	8.5	14[3]
Opaques[4]	9.5	6.0	13

[1]Mineral norms converted to vol.%
[2]PP consist of pyroxenes and plagioclase
[3]Very fine-grained intergrowths of sulfide (~70 vol.%) and pyroxene (~30 %)
[4]Include metal, troilite and chromite

$Fs_{19.7}Wo_{0.9}$) and very low birefringence) forming a sort of groundmass; a sulfide, usually troilite; metal; and olivine, the abundance of which varies considerably.

Two modes of occurrence of opaque minerals have been found in ORL: (1) as relatively large grains of metal and troilite; and (2) as very small troilite grains along the boundaries between large grains of olivine and pyroxene inside ORL, as well as at the boundary between ORL and CGL. The metal/sulfide ratio varies considerably. As a rule, the higher the troilite content, the higher the pyroxene/olivine ratio is in ORL.

Olivine also occurs in two types of grains: (1) as relatively large anhedral grains, similar in size to the other minerals; and (2) as small relict grains inside pyroxenes. The second type of olivine, characteristic of ORL, always shows reaction relations with the host pyroxene. In several cases, large anhedral olivine grains surrounded by ORL, and olivine grains within ORL, display the same optical orientation. Several grains of high-Ca pyroxene and whitlockite were found within some ORL domains.

Some of the larger regions of ORL, especially veins, display mineralogical zonation. An almost monomineralic pyroxene core becomes richer in opaque minerals and olivine toward the boundary with CGL. The silicates in ORL display undulatory extinction, and sometimes mosaicism in olivine.

Poikilitic Patches

Poikilitic patches (Figs. 1, 2) are composed chiefly of large anhedral grains of low- and high-Ca pyroxene, with rare plagioclase. In addition to large poikilitic grains, they contain numerous tiny (up to a dozen μm) inclusions and droplets of troilite and metal. Each poikilitic patch, as a rule, consists of several mineral grains, each a few mm in size. Sometimes high-Ca pyroxene forms corona-like rims around or within rounded grains of low-Ca pyroxene; and *vice versa*.

Pyroxenes often contain exsolution lamellae, the abundance of which varies considerably among grains. Both low- and high-Ca pyroxenes, when they are in contact with each other, contain relatively few lamellae. The greatest abundances of lamellae are found in PP, which are composed of only one pyroxene. Exsolved pyroxenes often contain a few small (tens of μm) euhedral poikilitic grains of another pyroxene having an optical orientation different from that of the exsolution lamellae. Exsolved augite ($Fs_{9.5}Wo_{45.3}$) in low-Ca pyroxene ($Fs_{24.3}Wo_{1.8}$) often forms relatively large (from some tens of μm to 350 x 150 μm) equidimensional or slightly elongated grains or blebs and rarely thin (<10 μm) lamellae parallel to perfect cleavage planes. Edges of some low-Ca pyroxene grains are depleted in the augite lamellae compared to the core, indicative of primary Ca zoning of the grains. In high-Ca pyroxene ($Fs_{10.2}Wo_{42.6}$), exsolved hypersthene ($Fs_{23.8}Wo_{1.5}$) forms a system of 5–12 μm-thick lamellae parallel to the grain elongation. A (rare) second system of lamellae, ~20 μm thick, is oriented at ~80° to the first.

Many clinopyroxene grains display undulatory extinction and well-developed planar fractures, which are very similar to those described by Stöffler *et al.* (1986) in the Shergotty meteorite. Orthopyroxene displays undulatory extinction and rare irregular fractures that are often filled by opaque minerals.

Several plagioclase-rich areas, up to 10 mm, have been found in the large section studied. In these areas (*e.g.*, Fig. 3) anhedral plagioclase grains, 0.5–2 mm, are associated with CGL olivine. Some plagioclase grains fill the space between euhedral olivine grains. Boundaries between olivine and plagioclase grains are generally smooth and straight. The plagioclase contains rare rounded poikilitic grains of other silicates, usually olivine, and small inclusions of opaque minerals in abundances much lower than in the other silicates. Some plagioclase grains display regular twinning, sometimes with diffuse boundaries between the twins. The area shown in Fig. 3 is crossed by a thick metal-sulfide vein containing fragments of silicates, including plagioclase. The vein clearly postdates its silicate host.

MINERAL CHEMISTRY

Silicates in the Divnoe meteorite display a complicated pattern of chemical variations both between lithologies and among separate mineral grains, as well as within mineral grains. While these variations were not observed in the earlier study of Divnoe (Zaslavskaya *et al.*, 1990), the mean compositions of minerals reported here are very close to those of Zaslavskaya *et al.* (1990).

Olivine

The mean compositions of olivine in CGL and ORL are listed in Table 2, and variations of Fe and Mg among separate grains as well as between lamellae in a single grain are shown in Fig. 6. While the compositional ranges of grains in CGL and ORL overlap, the difference between mean compositions is real. The ORL olivine is always more magnesian than olivine in neighboring CGL. Manganese, which is always detectable, displays minor deviations from the mean concentration and a weak positive correlation with Fe. The Fe/(Mg+Fe) ratio in Divnoe olivine is intermediate to those of ureilites and brachinites. The Ca content is very low, similar to that of olivine in terrestrial and lunar plutonic rocks (Warren and Kallemeyn, 1989). Olivine that is in contact with large chromite grains displays pronounced Cr zoning, with Cr content decreasing from the rim (up to 0.7 wt% Cr_2O_3) to essentially zero at the core.

Two other types of variations have been found within individual grains. These are normal large-scale (tens to hundreds of μm) Fe-Mg zoning, and superimposed fine-scale (several μm to some tens of μm) variations caused by the lamellar structure of the olivine (Fig. 7).

Large-scale zoning is usually observed in olivine grains where they are in contact with pyroxene; the Fe/(Mg + Fe) ratio increases toward the contact. The difference in Fa content between core and rim is usually less than 1 mol%, but sometimes it is as much as 3

TABLE 2. Mean compositions of Divnoe minerals

Mineral Lithology	Ol CGL	Ol ORL	Pl PP	Chr	Whit
No of analyses	81	37	47	64	3
SiO_2	37.42	37.96	59.81	0.04	n.d.
TiO_2	0.02	0.02	n.d.	0.96	0.03
Al_2O_3	0.01	0.01	26.29	9.87	n.d.
Cr_2O_3	0.06[1]	0.02	0.01	55.63	0.01
FeO	23.57	21.65	0.02	27.46	1.12
MnO	0.45	0.42	n.d.	0.55	0.02
MgO	38.68	39.92	0.01	3.95	3.43
CaO	0.02	0.03	7.50	0.01	46.71
Na2O	0.03	0.03	6.99	0.01	2.53
K2O	0.01	0.03	0.09	0.01	0.03
P2O5	n.d.	n.d.	n.d.	n.d.	45.71
Total	100.37	100.13	101.10	98.49[2]	99.58
Fa	25.48	23.33			
Fo	74.52	76.67			
An			37.02		
Ab			62.44		
Or			0.54		

[1]Contributed mainly by rim analyses with high Cr content
[2]Also contains ~0.7 wt.% each of V_2O_3 and ZnO (Zaslavskaya et al., 1990), which were not included in this analysis

mol%. However, in some cases very near the contact (up to few tens of μm), the trend reverses and the Fe/(Mg + Fe) ratio decreases slightly outward (Fig. 8).

Fine-scale variations in Mg and Fe caused by compositional difference between olivine lamellae are most pronounced in microprobe scans that are perpendicular to the lamellar structure. The range of variation in most of the microprobe scans executed is less than 3 mol% Fa. However, these points were uniformly spaced in the scans and not placed optimally according to tones in the BSE images. To define the compositional variability more precisely, the lightest (Fe-rich), darkest (Mg-rich), and some intermediate lamellae were analyzed in three olivine grains. Differences of 2.7, 3.0 and 3.2 mol% Fa were found (Fig. 9), as well as a strong positive correlation between Fe and Mn, the latter being the only significant (>0.05 wt%) minor element.

Pyroxenes

The mean compositions of a number of pyroxenes are listed in Table 3, and the variability of Fe, Mg, and Ca concentrations are shown in Fig. 10. Table 3 also lists the calculated primary compositions of the low-Ca pyroxene richest in Ca and the high-Ca pyroxene poorest in Ca. In general, pyroxenes in Divnoe are quite different from those of olivine-rich achondrites but are similar in composition to the pyroxenes in diogenites. Variations of minor elements in Divnoe pyroxenes do not show a regular pattern compared to other meteorites. Aluminum contents of both orthopyroxene and augite are similar with those of lodranites but lower than Al contents of brachinites, diogenites and ureilites. Both Cr and Ti are depleted in Divnoe pyroxenes compared to those in the meteorite groups mentioned above.

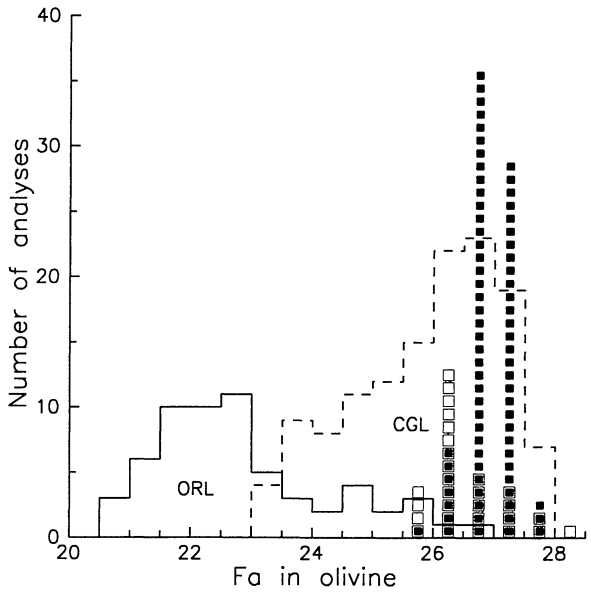

FIG. 6. Compositional variation in Divnoe olivines. Dashed line, CGL olivine; solid, ORL. Filled and open squares represent individual analyses from microprobe scans made within two separate lamellar grains. While olivine compositions of CGL and ORL olivines overlap, the bimodal distribution is real; ORL olivine is always more magnesian than olivine in neighboring CGL.

The compositional ranges of low-Ca pyroxenes in CGL and ORL overlap (Fig. 11), but as in the olivine, an ORL pyroxene is always more magnesian than a neighboring PP pyroxene. Also, mean ORL pyroxene is more magnesian then PP pyroxene. The concentrations of all minor elements except Mn are 2–4x less in ORL pyroxene than in CGL pyroxene (Table 3). Iron displays a good correlation with Ca, Al, and Cr. There is less correlation between Fe and Ti, and no correlation was found between Fe and Mn (Fig. 11).

High-Ca pyroxenes in PP and ORL (Table 3) display a distribution pattern of minor elements similar to that seen in low-Ca pyroxene, but the compositional difference between two high-Ca pyroxene grains studied in ORL is relatively large. Low-Ca pyroxenes in contact with olivine display a decrease in Fe/(Fe + Mg) ratio toward the contact (Fig. 8), accompanied by decreases in Ca, Al, Cr, and sometimes by increases in Mn. This is very similar to the chemical variations among PP and ORL orthopyroxenes.

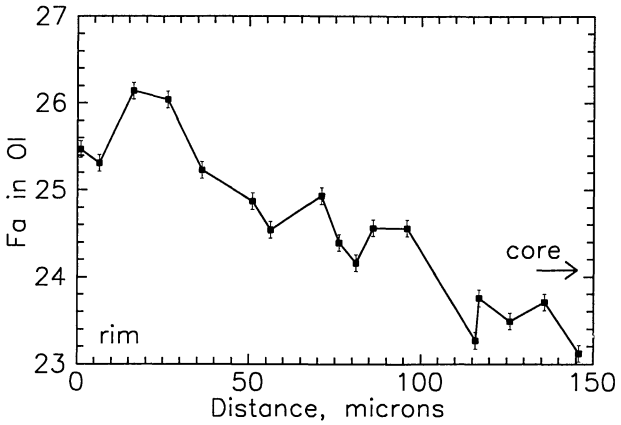

FIG. 7. Fine-scale variations in the fayalite content of olivine (*cf.* Fig. 4), which are superimposed on larger-scale variations.

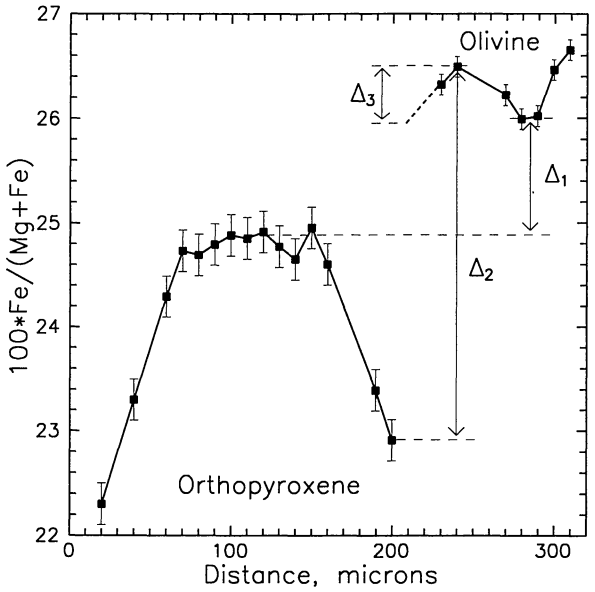

FIG. 8. Chemical zoning in adjacent olivine and pyroxene grains. The differences in Fe/(Mg + Fe) ratios (Δ_i) indicate primary equilibration of olivine and orthopyroxene at ~500 °C (Δ_1), and secondary heating of the meteorite to 700 °C (Δ_2). This was followed by relatively fast cooling, which decreased the Fe/(Mg + Fe) ratio only in olivine (Δ_3) because of the relatively slow diffusion of Fe and Mg in orthopyroxene.

Pyroxene that is in contact with large chromite grains displays Cr zoning similar to that found within olivine grains, but smaller in magnitude.

Plagioclase

The composition of this mineral (Table 2) is low in Or component and differs from that in most other meteorites. Only HED and mesosiderite plagioclases have such a low Or content, but they are also low in Ab, unlike Divnoe plagioclase. The range of

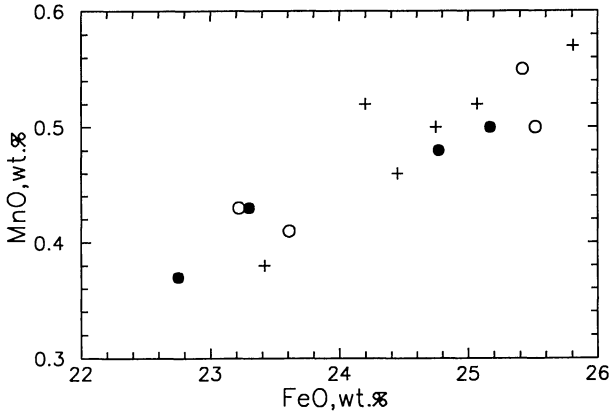

FIG. 9. Correlation between FeO and MnO concentrations in discrete olivine lamellae. Data for three separate grains are shown by different symbols.

Ab contents is similar to those of brachinites, shergottites and Chassigny, but the latter all have higher Or contents than Divnoe.

All plagioclase grains studied display regular igneous zoning, sometimes asymmetric, with 40–45 mol% An in grain cores and 32–37% An in rims. In large grains, the difference in An content between core and rim is 9–15 mol%. Two neighboring grains separated by a thick metal-troilite vein and an elongated olivine fragment (Fig. 3) display similar zoning patterns (Fig. 12), suggesting that intrusion of the vein displaced olivine which formerly lay between them.

Chromite

The mean composition of Divnoe chromite is shown in Table 2. Despite the substantial morphological diversity among chromite grains, their compositions are remarkably uniform and practically identical to that found in the previous study (Zaslavskaya *et al.*, 1990). Compared to chromite in other primitive achondrites,

TABLE 3. Mean compositions of pyroxenes in Divnoe

Mineral Opx Phase Lithology	Opx bulk PP	Aug bulk ORL	Aug bulk ORL	Opx bulk ORL	Aug host PP	Aug lam PP	Opx host PP	Pig* lam PP	Aug* bulk PP	bulk PP
No of analyses	19	76	1	1	41	40	19	22		
SiO_2	54.16	54.59	51.24	53.42	54.13	52.94	52.76	54.16	53.86	52.86
TiO_2	0.08	0.04	0.03	0.16	0.05	0.11	0.19	0.08	0.03	0.18
Al_2O_3	0.37	0.12	0.09	0.58	0.36	0.73	1.09	0.51	0.46	1.05
Cr_2O_3	0.23	0.06	0.32	0.34	0.21	0.71	0.91	0.25	0.34	0.86
FeO	15.56	14.88	6.13	4.87	15.95	6.01	6.27	16.04	15.26	6.98
MnO	0.45	0.46	0.21	0.20	0.45	0.23	0.22	0.47	0.43	0.24
MgO	27.57	28.76	17.68	16.68	27.76	16.08	16.30	28.18	25.40	17.16
CaO	0.92	0.51	22.03	23.88	0.93	22.42	20.49	0.81	3.77	19.07
Na_2O	0.03	0.02	0.11	0.28	0.01	0.38	0.42	0.02	0.06	0.39
K_2O	0.01	0.01	n.d.	n.d.	n.d.	n.d.	n.d.	n.d.	n.d.	n.d.
Total	99.39	99.47	98.26	100.72	99.35	98.91	98.91	100.55	99.28	98.79
Fs	23.58	22.28	9.31	7.47	24.28	9.47	10.18	23.83	23.30	11.26
En	74.65	76.78	47.85	45.61	73.82	45.22	47.19	74.62	69.18	49.36
Wo	1.77	0.98	42.85	46.92	1.80	45.30	42.63	1.54	7.51	39.41

*Calculated bulk compositions of low-Ca (Pig) and high-Ca (Aug) primary pyroxenes

Divnoe chromite is depleted in MgO and to a lesser extent in TiO_2 and MnO, but enriched in Al_2O_3 (~2 wt%).

Whitlockite

Three grains from different lithologies have essentially the same composition. Their average composition (Table 2) is close to that of whitlockite in ordinary chondrites.

Metal and Sulfides

Detailed chemical and structural studies of large metal and sulfide grains were made by Zaslavskaya *et al.* (1990) and are beyond the scope of this work. Only a few analyses were performed, with results which are in good agreement with those of the previous study. Special attention was paid to small inclusions of these minerals in olivine and pyroxenes as well as in the layers separating mineral grains in CGL.

Droplet-like opaque inclusions in silicates are usually too small for quantitative analysis, so these phases were usually identified on the basis of maps of Fe, Ni, and S X-ray intensity. It was qualitatively apparent that metal and troilite inclusions in pyroxenes are enriched in Ni; this is consistent with the results of quantitative analyses performed on a few of the larger inclusions. Metal inclusions in olivine, on the other hand, have the same compositions as large metal grains (Zaslavskaya *et al.*, 1990). Opaque veins or layers between separate silicate grains in CGL usually consist of troilite or Ni-free iron oxides; no Ni-free metal grains were found.

MINERAL THERMOMETRY

The structure and mineral chemistry of Divnoe are indicative of a complicated and prolonged thermal history, the nature of which may be inferred by the use of several known mineral thermometers.

Olivine-orthopyroxene Thermometer (Sack and Ghiorso, 1989)

The diagram in Fig. 13 (calculated by R. O. Sack, pers. comm.) shows the equilibrium distribution of Mg and Fe between coexisting olivine and orthopyroxene at 1 bar, along with data for olivine-orthopyroxene pairs in CGL and ORL. A prominent feature of the diagram is the closeness of data points for the cores of Divnoe minerals to the 500 °C isotherm, which implies equilibration between olivine and orthopyroxene at this low temperature during slow subsolidus cooling. Among CGL olivine-orthopyroxene pairs, only rim compositions of coexisting olivine and pyroxene correspond to a higher temperature (600–700 °C).

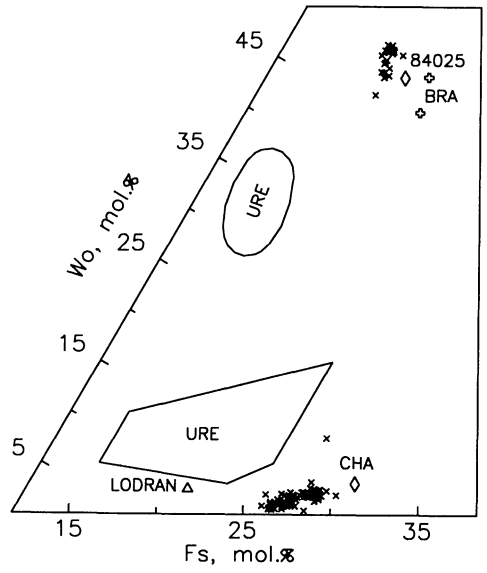

FIG. 10. Divnoe pyroxenes (X) differ in composition from most meteoritic pyroxenes, including those of all known primitive achondrites, but they exactly match diogenite pyroxenes (not shown). Data from Warren and Kallemeyn (1989) and Takeda *et al.* (1988).

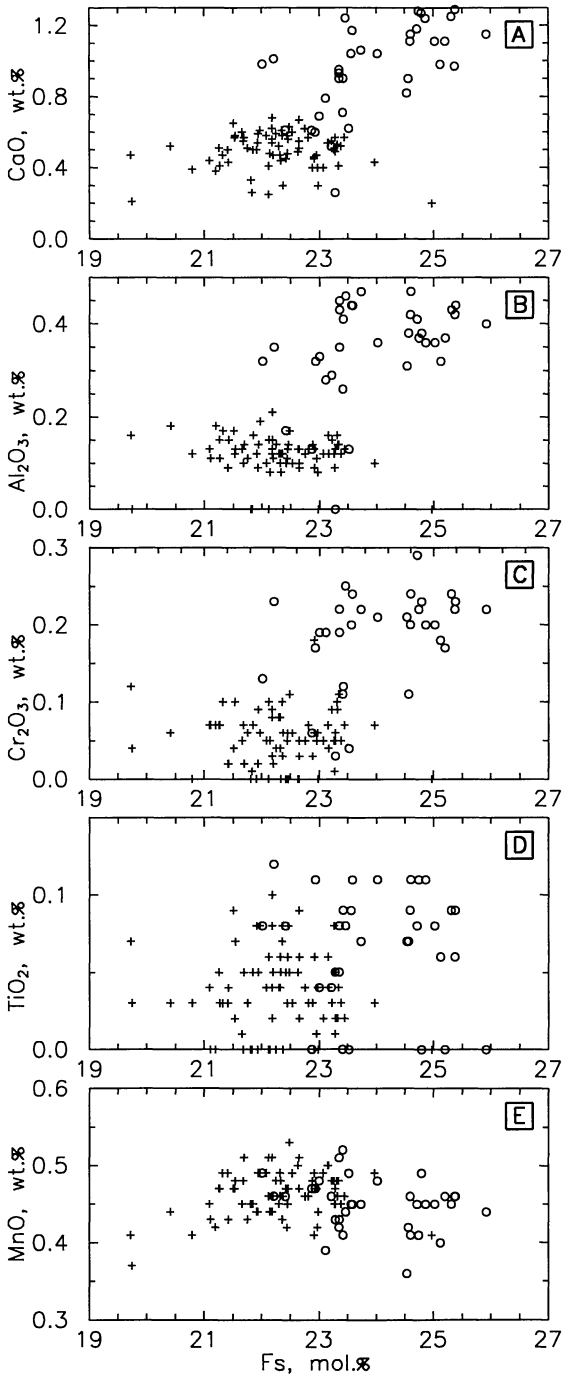

FIG. 11. Minor element concentrations in Divnoe low-Ca pyroxenes, as a function of Fs. Open circles, PP pyroxenes; crosses, ORL pyroxenes. The ORL pyroxene is depleted in all minor elements, except Mn, compared to PP pyroxenes. The degree of depletion correlates negatively with Fs content.

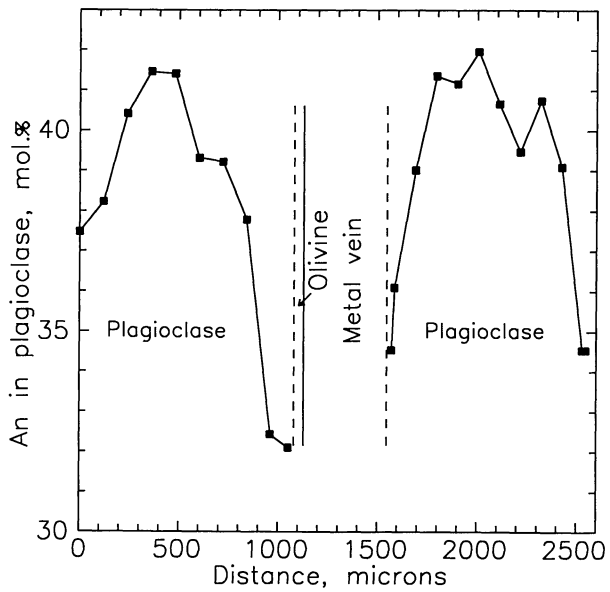

FIG. 12. Compositional zoning in two plagioclase grains separated by fragment of olivine grain and thick metal-sulfide vein shown in Fig. 3.

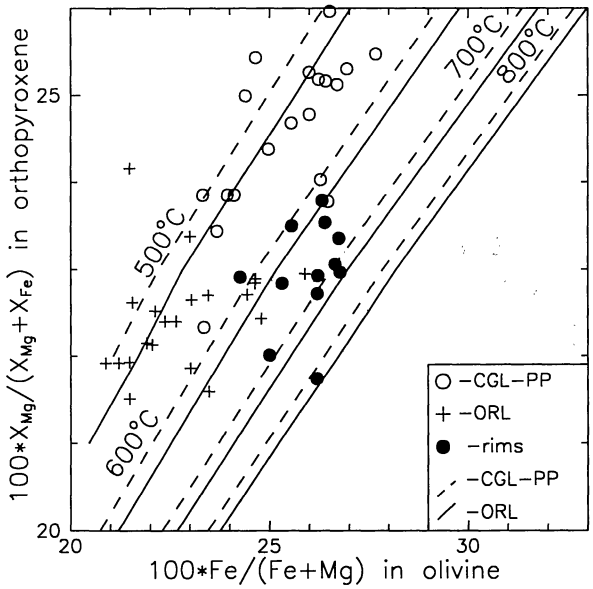

FIG. 13. Application of the olivine-orthopyroxene thermometer (Sack and Ghiorso, 1989) to Divnoe. Dashed (2 mol% Wo in opx) and solid (1 mol% Wo in opx) curves are isotherms for CGL and ORL, respectively. Compositions of olivine and orthopyroxene coexisting in ORL, CGL, and PP plot roughly along the 500 °C isotherm. Only the compositions of olivine and orthopyroxene rims deviate from this isotherm, implying a reheating event. Deviations of some ORL ol-opx pairs from this isotherm are due to the more ferrous compositions of some large olivine grains which appear to be associated with ORL, but have compositions similar to those of neighboring grains in CGL.

The deviation of some ORL mineral pairs from this isotherm may result from misunderstanding of the affiliation of some relatively large olivine grains near boundaries between ORL and CGL: the grains appear to be associated with ORL, but have compositions similar to those of neighboring grains in CGL.

The Olivine-chromite and Orthopyroxene-chromite Thermometers

Three other mineral thermometers have been used to calculate equilibrium temperatures in Divnoe: the ol-chr thermometer of Jackson (1969), which has been most often used in meteorite studies; and two recently calibrated thermometers, the ol-chr thermometer of Sack and Ghiorso (1991) and the opx-chr thermometer of Mukherjee *et al.* (1989). Temperatures derived from Jackson's thermometer (~1300 °C) are ~400° higher than those of Sack and Ghiorso (R. O. Sack, pers. comm.) (895 ± 17 °C, Fig. 14) and, even more important, ~500° higher than the temperature for the opx-chr pair coexisting with the same olivine grain. Opx-chr temperatures (Fig. 14) are ~100° lower (mean = 777 ± 25 °C) than those derived from the ol-chr thermometer, even for coexisting grains of olivine, orthopyroxene, and chromite. Thus, there appears to be a nonequilibrium distribution of Mg and Fe among these three minerals.

The Orthopyroxene-clinopyroxene Thermometer.

The diversity of morphological types of pyroxenes in Divnoe provides a good opportunity to estimate the temperatures of both intergrain and intragrain pyroxene equilibration as well as that of crystallization from the melt. The many two-pyroxene thermometers have been reviewed recently by Fonarev and Graphchikov (1991). Two thermometers were used in the present study: the "graphic" thermometer of Lindsley and Anderson (1983) and the "analytical" thermometer of Fonarev and Graphchikov (1991). These give similar results at temperatures above 900 °C, but at lower temperatures the "analytical" thermometer has smaller uncertainty.

The "analytical" thermometer permits the estimation of temperatures based on two different reactions: the intercrystalline distribution of Fe and Mg between coexisting ortho- and clinopyroxenes, and the intracrystalline distribution of Ca, Fe and Mg within clinopyroxene. The two temperatures should be the same if complete equilibrium is attained. The data for PP pyroxenes (Fig. 14) yield mean temperatures of 744 ± 53 °C ("intergrain") and 825 ± 24 °C ("intragrain"), suggesting a lack of complete equilibration between the lamellae and host pyroxenes in low- and high-Ca pyroxenes. While the mean temperatures are in agreement to within an uncertainty that incorporates the data scatter and the uncertainty of the thermometers themselves, each particular pair of coexisting ortho- and clinopyroxene grains gives a ~100° difference between "intragrain" and "intergrain" temperatures. This difference could result from a cooling rate at temperatures below ~850°C which was slow enough to equilibrate the concentrations of small Fe^{2+} and Mg^{2+} cations but not large Ca^{2+} ions.

The "graphic" thermometer and compositions of primary pyroxene grains (Table 3) have been used to estimate igneous temperatures. The temperatures found, ~1150 °C (low-Ca px) and ~1100 °C (high-Ca px), differ slightly from one another, but are within the uncertainty range (~70°) of this thermometer for magnesian high-Ca pyroxene (Fonarev and Graphchikov, 1991).

The Troilite-metal Thermometer

Experimental data for this rarely-used thermometer have been presented by Bezmen *et al.* (1978), and coefficients for the equation describing the equilibrium distribution of Ni between troilite and taenite are from Petaev *et al.* (1990a). While this thermometer is not very precise, it is used here because metal and

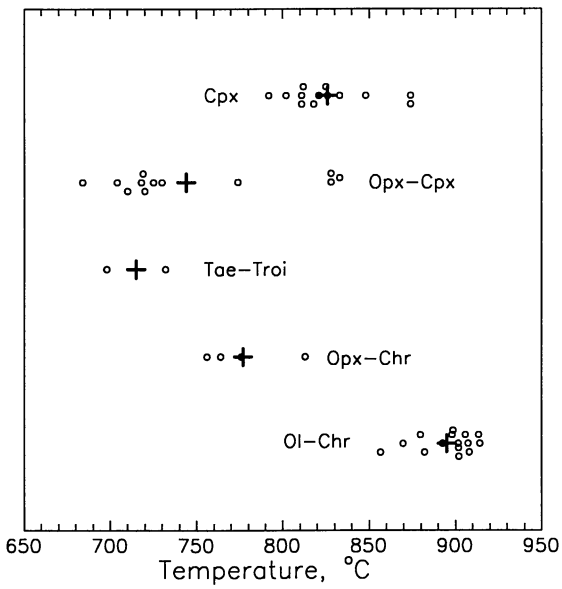

FIG. 14. Distribution of equilibrium temperatures for Divnoe derived from five different thermometers: Ol-Chr (Sack and Ghiorso, 1991); Opx-Chr (Mukherjee *et al.*, 1989); Opx-Cpx and Cpx - "intergrain" and "intragrain" two-pyroxene thermometers, respectively (Fonarev and Graphchikov, 1991); Tae-Troi (Bezmen *et al.*, 1978). The vertical scale is used only to separate the data for discrete mineral pairs. Open circles show temperatures derived for particular pairs of grains; crosses show the mean temperatures derived from each thermometer. The disagreement between thermometers probably results from different "closure temperatures" for the various thermometers, beneath which diffusion of the elements, on which each thermometer depends, becomes too slow for equilibrium partitioning to be maintained (see discussion in text).

troilite are able to equilibrate at lower temperatures than silicates. Calculations could be carried out for only two troilite-taenite pairs found in inclusions in olivine and high-Ca pyroxene. The equilibrium temperatures found (Fig. 14), 732 °C (an inclusion in pyroxene) and 698 °C (an inclusion in olivine), are close to those calculated for "ol-opx" rims but much higher that of the "ol-opx" isotherm. Since troilite and metal are able to equilibrate to lower temperatures than silicates, the higher temperatures recorded by these minerals than their host silicates must be attributable to a secondary heating event that was too brief to affect more than the rims of the host silicates.

Thermal History

The compositions of primary low- and high-Ca pyroxenes as well as the meteorite texture suggest that it was heated to temperatures greater than 1150 °C, where melting occurred; then it cooled slowly to ~500 °C, as is indicated by the "ol-opx" thermometer. The apparent disagreements between the "ol-chr", "opx-chr," and two-pyroxene thermometers result from a cooling rate which at temperatures of 800–850 °C was too fast to permit equilibration of Mg and Fe between chromite and silicates, and Ca between ortho- and clinopyroxene as well as within plagioclase. But it was slow enough to allow equilibration of Mg and Fe between olivine and orthopyroxene. Since the difference in the equilibrium Fe/(Mg + Fe) ratios of olivine and orthopyroxene decreases with temperature, low-temperature re-equilibration of olivine and orthopyroxene could result in overestimation of the "ol-chr" temperature and, at the same time, underestimation of the "opx-chr" temperature. This would allow reconciliation of the "ol-chr" and "opx-chr" temperatures with the two-pyroxene "intragrain" temperature.

The fact that the difference in Fe/(Mg + Fe) ratios between coexisting olivine and orthopyroxene rims (Δ_2 in Fig. 8) is greater than that of equilibrated core compositions (Δ_1) clearly indicates that a secondary heating event raised the temperature to ~700 °C, which also re-equilibrated the metal and troilite within small inclusions. The system must have cooled relatively rapidly, to preserve the observed compositions of metal and troilite and the silicate rim compositions. The Fe content of the outermost rims of olivine grains decreased slightly (Δ_3) during cooling; pyroxene grain rims were not affected because of the smaller Fe diffusion coefficient in pyroxenes.

TABLE 4. Oxygen isotope compositions of Divnoe samples

Sample	$\delta^{18}O$	$\delta^{17}O$	$\Delta^{17}O$
Fine-grained powder	4.74	2.24	-0.23
Coarse-grained powder	4.92	2.38	-0.18
Chip	5.05	2.29	-0.34
Bulk, nonmagn.fraction	4.65	2.23	-0.18
Ol-rich chip	4.43	1.84	-0.47
Olivine separate	4.79	2.32	-0.17
Pyroxene separate	5.07	2.39	-0.25

OXYGEN ISOTOPES

Oxygen isotope data for a number of samples and mineral separates are listed in Table 4 and shown in Fig. 15. With the exception of one somewhat aberrant analysis, all samples have uniform isotopic compositions, allowing for a normal mass-dependent fractionation between pyroxene and olivine, which is on the order of 0.3 to 0.4‰ in $\delta^{18}O$ at igneous temperatures (Anderson *et al.*, 1971). Our data agree with the earlier oxygen

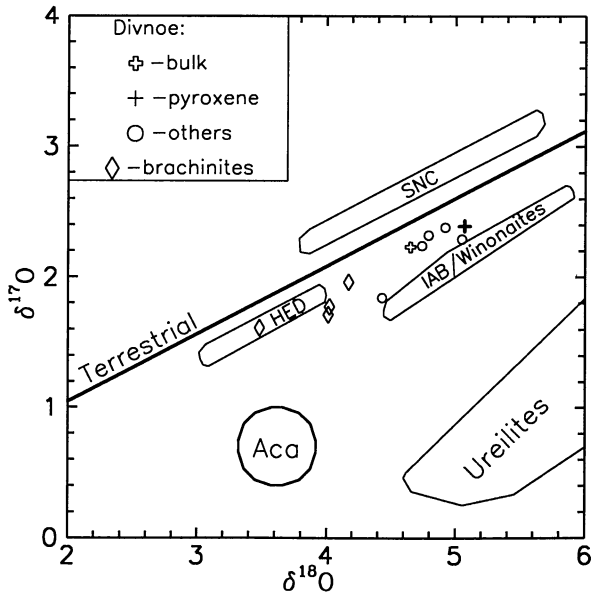

FIG. 15. Oxygen isotope compositions of Divnoe samples. Bulk sample (Swiss cross) is an aliquot of the non-magnetic fraction. HED = howardites, eucrites, diogenites; SNC = shergottites, nakhlites, Chassigny; Aca = acapulcoites/lodranites. With the exception of one somewhat aberrant analysis, the bulk sample, a pyroxene mineral separate, and several chips fall in a narrow range, with $\Delta^{17}O = -0.26$. On the basis of oxygen isotopes, Divnoe has no affinity to any known meteorite group. Data from Clayton and Mayeda (1992).

isotope analyses of Divnoe by Zaslavskaya *et al.* (1990) in $\Delta^{17}O$, but are systematically higher in $\delta^{18}O$ and $\delta^{17}O$. This difference may be due, in part, to a different definition of the SMOW standard. It may also be a consequence of fractionation during the "selective fluorination procedure" used by Zaslavskaya *et al.* (1990).

The oxygen isotopic compositions do not correspond exactly with any of the previously recognized chondritic or achondritic groups (Clayton, 1993). The value of $\Delta^{17}O$ for Divnoe is = −0.26 ± 0.11, which falls within the ranges for HED meteorites (−0.26 ± 0.08) and for brachinites (−0.28 ± 0.09) (Clayton and Mayeda, pers. comm.) and is resolvable from the range for the IAB/winonaite group (–0.46 ± 0.09). However, the $\delta^{18}O$ values for Divnoe are about 2‰ higher than olivine-rich members of the HED group, and about 1‰ higher than members of the brachinite group (Nehru *et al.*, 1992). The brachinites are currently represented by only four meteorites (ALH 84025, Brachina, Eagles Nest, and Nova 003), so the range of isotopic variability within the group is not well-defined. Thus, the oxygen isotopic composition of Divnoe might be compatible with differentiation from a brachinite source material, but it is incompatible with genetic relationships with other known reservoirs, such as IAB/winonaites, HED, acapulcoites/lodranites, and ureilites.

BULK CHEMISTRY

Major and trace element data for bulk samples and the non-magnetic fraction of Divnoe are shown in Table 5, with data for some texturally or isotopically similar meteorites for comparison. In general, the concentrations of major and minor elements measured in this study are close to those found by Zaslavskaya *et al.* (1990) except for slightly higher metal and lower normative high-Ca pyroxene in our sample. Since the total weight of our sample is almost 4x greater than that of any bulk sample previously studied, our analyses should be the most representative of the Divnoe meteorite as a whole. Comparison of the composition of Divnoe with those of other olivine-rich meteorites (Table 5) reveals broad similarity, except that most incompatible elements are depleted in Divnoe relative not only to chondrites but also to the differentiated meteorites listed in Table 5.

The data on alkalies in Table 5 require comment. Alkalies and Al in the bulk sample both occur in the same silicate minerals ($NaAlSi_2O_6$ dissolved in pyroxenes, and $(Na,K)AlSi_3O_8$ dissolved in plagioclase); Al is also present in chromite. As was also found by Zaslavskaya *et al.* (1990), the Na_2O and K_2O contents in our bulk sample (0.75 wt% and 0.10 wt%, respectively) are implausibly high relative to the Al abundance of the sample. Therefore, the Na_2O and K_2O concentrations we present in Table 5 were calculated from the mineral norms provided by the analysis (Table 6) and by observed mineral chemistry (Tables 2 and 3).

To calculate mineral norms, the measured compositions of minerals were assumed to be representative and mineral abundances were calculated in the following sequence: chromite (from the Cr_2O_3 concentration), whitlockite (from P_2O_5), plagioclase (from residual Al_2O_3), high-Ca pyroxene (from residual

TABLE 5. Bulk chemistry of Divnoe (Di) and some olivine-rich meteorites (wt.%)

		Di, bulk	Di,chip[1]	Acap[2]	Ure[3]	Bra[4]	Cha[5]	IAB[6]	Lodr[7]
SiO_2		34.93		37.44	36.60	36.37	38.17	40.52	34.90
TiO_2		0.025		0.13	0.11	<0.027	0.10	0.13	0.05
Al_2O_3		0.40		2.25	0.52	0.17	0.70	1.64	0.90
Cr_2O_3		0.49	0.89	1.08	0.59	0.58	0.63	0.30	0.81
FeO		16.41		6.38	17.94			3.33	11.54
MnO		0.34	0.38	0.38	0.35	0.33	0.53	0.31	0.42
MgO		29.01		24.71	34.47	30.51	31.61	31.94	29.53
CaO		1.39	1.3	1.57	0.99	2.52	0.60	2.48	1.54
Na_2O		0.093*	0.039	0.83	0.20	0.07	0.13	0.47	0.21
K_2O	(ppm)	11*	5	520	240	<50	410	720	<240
P_2O_5		0.09		0.08	0.08		0.06	0.03	0.49
H_2O^+		0.26			3.19**				
H_2O^-		0.45			0.30			0.12	0.04
FeS		4.38		3.60	1.95			1.32	2.10
Fe_{met}		10.31		20.34	0.21			0.25	14.28
Ni		0.82	0.73	2.195	0.21	0.51	0.05	0.10	1.13
Co		0.061	0.057	0.034	0.011	0.04	0.01	<0.01	0.07
Cu		0.014				0.005			
C		0.12						0.08	
Fe_{tot}		25.85	25.10	27.5		25	21.07	3.68	31.20
Total		99.64		101.79	97.54	96.13	93.78	100.17	98.03

*Calculated from normative mineralogy
**Also includes C and other volatiles released up to 1100°C
[1]Data from (Wasson and Kallemeyn, 1992; *pers. comm.*)
[2]Acapulco (Palme *et al.*, 1981)
[3]Ureilite Y790981 (Takeda, 1986)
[4]Brachinite ALH 84025 (Warren and Kallemeyn, 1989)
[5]Chassigny (Treiman *et al.*, 1986)
[6]Silicate inclusion from the El Taco iron (Jarosewich, 1990)
[7]Lodranite Y-791493 (Nagahara and Ozawa, 1986)

TABLE 6. Normative composition of Divnoe (wt.%)

Mineral	Content
Olivine	69.60
Orthopyroxene	10.26
Clinopyroxene	2.61
Plagioclase	1.10
Whitlockite	0.13
Chromite	0.71
Metal	11.21
Troilite	4.38

CaO), and olivine + low-Ca pyroxene with the same Mg/(Mg+Fe) ratio. Such a calculation does not take Na_2O and K_2O contents into consideration, and neglect of the Al_2O_3 content of the pyroxenes results in a 10–15% increase in the plagioclase abundance. The bulk abundance of K calculated by this procedure is of the same magnitude as the mass-spectrometrically measured concentration of K in two separate chips (2.3 and 3.2 ppm; Petaev *et al.*, 1992) and the INAA value for K in another 309 mg Divnoe chip (Table 5; J. T. Wasson and G. W. Kallemeyn, pers. comm.), though it is much lower than the INAA value for K (87 ppm) found for an aliquot of the non-magnetic fraction (G. W. Kallemeyn, pers. comm.). The INAA value for Na (302 ppm) in this aliquot is also considerably higher than those calculated from the mineral norms and measured in a separate chip (Table 5).

The variations in Na and K contents correlate positively with LREE contents in the same samples (Fig. 16). Again, LREE contents calculated from the mineral norms (Table 6) and the REE concentrations measured in Divnoe minerals (Davis *et al.*, 1993; A. M. Davis, pers. comm.) are slightly higher than those in the small chip. These LREE are much lower than values for the aliquot of non-magnetic fraction as well as for the previously studied bulk samples (Zaslavskaya *et al.*, 1990). Such a large difference between calculated and measured Na, K, and REE contents could either reflect heterogeneity of the bulk sample studied or a presence of a small amount of K, Na, LREE -rich component like that found by Bild and Wasson (1976) in Lodran and are not included in our calculations. The former seems not to be the case, since trace element contents in two different aliquots of non-magnetic fraction analyzed in two different laboratories by different techniques (INAA and RNAA) are in a good agreement (Table 7). The only possible component beyond the minerals found in our extensive study (Table 6) is terrestrial weathering products. If a weathering component enriched only in the most incompatible elements were present, it might be able to explain the observed differences since a larger, less-carefully-chosen sample would contain more weathering products.

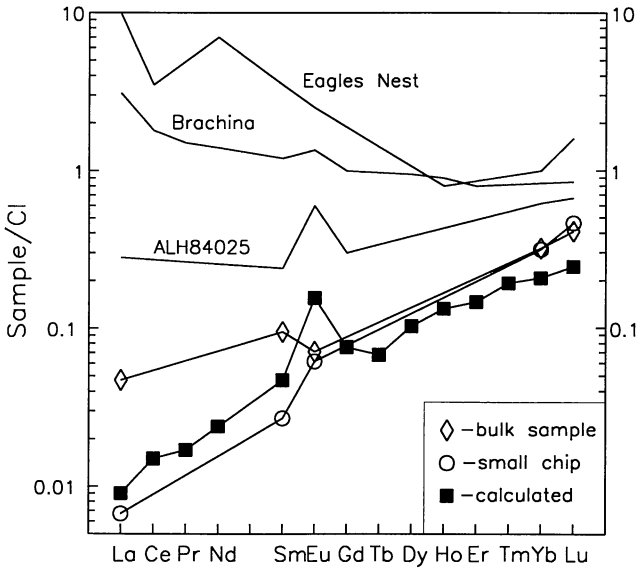

FIG. 16. The REE patterns in Divnoe samples: an aliquot of the bulk sample (G. W. Kallemeyn, pers. comm.); an integral chip (J. T. Wasson and G. W. Kallemeyn, pers. comm.); and bulk Divnoe, calculated from normative mineralogy. These imply crystallization from a fractionated melt depleted in LREE. The Divnoe REE patterns are quite different from those of brachinites (Nehru *et al.*, 1983; Warren and Kallemeyn, 1989; Kring and Boynton, 1992).

The trace element data for the two Divnoe samples (non-magnetic and whole-rock) are listed in Table 7, together with results for ALH A81187 acapulcoite, Y790981 (a ureilite irradiated and treated simultaneously with the Divnoe whole-rock sample) and two brachinites (Brachina itself: Nehru *et al.*, 1983; and ALH 84025: Warren and Kallemeyn, 1989).

Since Divnoe is a unique find, due caution must be exercised in considering trace element data for it, because compositional alteration could have occurred during its terrestrial residence. Two lines of evidence suggest that compositional alteration of Divnoe was not serious.

First, there is the matter of internal consistency: the composition of the non-magnetic portion is consistent with trends expected after removal of metal from Divnoe whole-rock (Table 7). Relative to whole-rock, the non-magnetic portion is enriched in lithophiles (U, Rb, Cs) and depleted in siderophiles (Au, Co, Ga, Sb, Ag?). The more labile trace elements show scattered trends consistent with their being dispersed elements: half (Se, Bi, Tl, In) have higher contents in the non-magnetic portion and half (Ag?, Te, Zn, Cd) have lower contents. (The concentrations of Ag are consistent either with siderophilic or labile behavior.)

Second, the composition of Divnoe whole rock grossly resembles the compositions of primitive achondrites, with no evidence for significant contamination. Of the meteorites listed, Divnoe most closely resembles the ureilite Y790981 chemically, although clearly it is not a ureilite. Divnoe contains 3x more Au and Co than Y790981, 1/10 the U, Rb and Cs, and 0.13–0.3x the Bi, Tl and In. However, the last trace elements are highly labile, and their concentrations often vary widely in meteorites. Most elements (Cd excepted) are much more abundant in the acapulcoites (Biswas *et al.*, 1981). Concentrations of a few elements in Divnoe whole-rock (especially Ag, Se, Zn and Cd) are comparable to or exceed those of ALH A81187 acapulcoite.

On the whole, then, we can say that trace element concentrations in Divnoe lie at achondritic levels and seem unaltered by terrestrial weathering. This conclusion does not support the notion of terrestrial contamination of Divnoe; thus, the cause of the observed variations in alkalies and REE contents remains unclear.

A comparison between Divnoe and brachinites is of special interest here, since only they among all known meteorites might be derived from a common oxygen reservoir. Contents of the major elements are quite similar (Table 5), indicative of the primitive achondritic nature of both Divnoe and brachinites, with Divnoe being slightly enriched in Ni and Co and having the higher MgO/(MgO + FeO) ratio. However, trace elements display quite different patterns. Divnoe is considerably depleted in REE, especially LREE, relative even to the highly differentiated ALH 84025, which contains no plagioclase (Fig. 16), indicative of either a nonchondritic primary composition of the Divnoe source region, or removal of the earliest partial melt generated before crystallization of pyroxenes, plagioclase, and whitlockite. Refractory siderophile contents, in contrast to REE, are ~3x higher in Divnoe than in brachinites (Table 7), while the bulk Fe contents are essentially the same in these meteorites. Since no significant amount of Fe has been removed from the brachinites, their depletion in siderophiles is strong evidence against a common precursor material for Divnoe and the brachinites.

TABLE 7. Trace elements in Divnoe and olivine-rich meteorites

El-t (*unit*)	1	2	3	4	5	6	7
Sc (*ppm*)	(6.7)	8.94				12	13.6
Zn (*ppm*)	133(144)	150	178	222	99.9	313	164
Ga (*ppm*)	2.78(2.5)	3.93	4	2.94	7.32	7.6	2.1
As (*ppm*)	(0.506)		1.31			0.18	0.55
Se (*ppm*)	4.65(4.22)	3.30	4.62	2.70	2.12	3.5	12.4
Br (*ppb*)	(0.553)					0.49	0.33
Rb (*ppb*)	127	8.48	236	399			
Ru (*ppb*)	(155)		776				
Ag (*ppb*)	18.3	24.5		22.0	14.5		
Cd (*ppb*)	5.99	27.6		25.0	7.55		
In (*ppb*)	0.48±0.06	0.14±0.05		1.08±0.08	2.07±0.10		
Sb (*ppb*)	0.58	26	38	23	130		56
Te (*ppb*)	74.5	143		251	1108		
Cs (*ppb*)	2.29	0.66		6.88	37.6		
La (*ppb*)	(11)		3			220	65
Sm (*ppb*)	(14)		7			190	34
Eu (*ppb*)	(4)		6			70	33
Yb (*ppb*)	(52)		78			220	98
Lu (*ppb*)	(10)		17			36	16
Os (*ppb*)	(113)		720				250
Ir (*ppb*)	(104)		692			135	132
Au (*ppb*)	51.9(46)	127	150	43.3	177	12.6	61
Tl (*ppb*)	0.74±0.28	0.17±0.02		0.66±0.03	12.9		
Bi (*ppb*)	2.53	0.79±0.06		2.57	3.53±0.15		
U (*ppb*)	3.50	0.13±0.02		1.53	8.88		

1 Divnoe, nonmagnetic fraction, our data; data by G.W.Kallemeyn (*pers.comm.*) are listed in parentheses
2 Divnoe, separate chip, our data
3 Divnoe, separate chip (J.T. Wasson and G.W. Kallemeyn, 1992; *pers. comm.*)
4 Ureilite Y790981, our data
5 Acapulcoite ALH A81187, our data
6 Brachina (Nehru *et al.*, 1983)
7 ALH 84025 (Warren and Kallemeyn, 1989)

DISCUSSION

The chemistry and mineralogy of Divnoe clearly indicate the important role of igneous processes in its evolution. This is in a good agreement with the conclusion reached by Zaslavskaya *et al.* (1990), that Divnoe is a sample of an originally subchondritic source region which has experienced partial melting, followed by crystallization of a portion of the melt *in situ* and removal of the rest of the melt in connection with a catastrophic event.

The petrological data presented above point to formation of the various Divnoe lithologies within the same source region but by different processes. The granoblastic nature of the CGL host lithology implies a more important role for solid state recrystallization than crystallization from the melt. The PP minerals, on the other hand, crystallized from a melt with poikilitic olivine grains being the first phase to crystallize. Low- and high-Ca pyroxenes crystallized almost simultaneously and reacted with both poikilitic and CGL olivine grains. Plagioclase was the last silicate phase crystallized. The ORL was formed by reaction between CGL olivine and a silicate melt enriched in opaque minerals before the crystallization of PP minerals. The ubiquitous troilite veins found in the meteorite suggest an extreme mobility of S, and the important role of this element in the Divnoe source region.

Primary Composition of the Source Region

The concentrations of some lithophile and siderophile elements in different samples, including those previously studied by Zaslavskaya *et al.* (1990), are in a good agreement with one another, and can be used to estimate the chemistry of the source region. The high Fe and S contents of Divnoe point to a chondritic composition for the precursor material of the meteorite. The high U/Rb, U/Cs, Os/Au, and Os/Ga ratios suggest that the source region was enriched in refractory elements (Sc, Os ~1.5x CI, Ir 1.4x CI), common elements (Co ~1.2x CI), and even some moderately volatile elements (Au ~1.1x CI); and depleted in more volatile elements, with the depletion increasing with volatility (Ga ~0.4x CI, Bi ~0.007x CI). At the same time, the U/Os (~0.27x CI), U/Sc (~0.26x CI), Ti/Sc (~0.23x CI), and Al/Sc (~0.16x CI) ratios indicate substantial loss of incompatible elements, probably due to removal of partial melt.

Removal of a low-temperature silicate melt fraction could also be accompanied by the loss of a metal-sulfide melt and the depletion of Divnoe in Ni (Ni/Fe and Ni/Co are ~0.6x CI) and, to a lesser degree, in S. However, depletion of the meteorite in sulfur, caused by its removal as partial melt, seems to be insignificant. While S/Fe in Divnoe is relatively low (0.19x CI), the depletion of

the meteorite in S relative to its cosmic abundance is caused by a primary depletion of the source region in volatile elements (Ga/Co = 0.35x CI, Sb/Co = 0.23x CI, Se/Co = 0.22x CI) rather than by its removal as a melt. The high ratios of chalcophile to siderophile elements of similar volatility (Se/Ga = 0.62x CI and Se/Sb = 0.93x CI) do not indicate a substantial removal of chalcophiles relative to siderophiles.

Thermodynamic Model

To estimate the amount of unmelted residue after partial melting and the amount of partial melt that crystallized *in situ*, we carried out a thermodynamic analysis of melting and crystallization in a system having the composition of Divnoe. The calculations used the LUNAMAG code (Ariskin *et al.*, 1991, 1992;) developed originally for modelling the origin of lunar basalts. The program calculates phase relations in a "solids-melt" system based on experimental data for the distribution coefficients of major (Si, Ti, Al, Fe, Mn, Mg, Ca, Na, K and P) and some trace elements. Input parameters were the concentrations of rock-forming oxides (except Cr_2O_3) plus pure iron converted to FeO, the oxygen fugacity, and the degree of crystallization or melting. Output from the calculations are an equilibrium temperature, the abundances and compositions of minerals and melt, and the bulk distribution coefficients of trace elements between solid phases and melt.

In a system having the composition of Divnoe (Table 5 minus Cr_2O_3, Ni, Co, FeS and H_2O), only olivine, metal, and melt are in equilibrium at degrees of melting greater than 10 wt%. The metal content of the residue and the FeO contents of olivine and the melt depend upon oxygen fugacity and the degree of melting. By varying the oxygen fugacity assumed in the calculations, we found that at $\log(fO_2)$ = IW-1.8 (1.8 log unit below the iron-wüstite buffer), the olivine composition (Fa_{26}) and metal content (~10 wt%) are close to those in Divnoe. This equilibrium occurs at 1311 °C; the assemblage contains, in addition to metal, 79 wt% olivine and ~11 wt% melt enriched in FeO, MgO and CaO (Table 8, column 1).

Since the chemical data clearly point to a chondritic primary composition for the Divnoe source region, we also modelled partial melting in systems having chondritic (LL), primitive achondritic (Acapulco and Y74063) and chondrule-like (ferromagnesian Allende chondrules) compositions. The best agreement between model results and the Divnoe mineralogy was found for an Acapulco-like composition.

In a source region of Acapulco composition, omitting (as in the Divnoe case) Cr_2O_3, Ni, Co, and FeS, at 1304 °C and at the oxygen fugacity derived above (IW-1.8), the equilibrium assemblage consists of 70.7 wt% olivine (Fa_{23}), 8.7% metal, and 20.6% melt enriched in Al_2O_3, FeO, CaO, and Na_2O (Table 8, column 2). In such a source region, the abundances of olivine and metal are close to those in Divnoe.

We also calculated the products of crystallization from the partial melt found above, at the same oxygen fugacity and assuming the melt does not react with the residue. The crystallization of partial melt starts with olivine and free metal (Fig. 17a). Three to four wt% of the latter is stable over the entire range of temperatures considered. After the crystallization of 18% of the melt (at 1159 °C), augite appears. Just after this (1156 °C), the melt begins to react with the olivine to form low-Ca pyroxene. These temperatures are very close to those derived from the two-pyroxene thermometer. The first low-Ca pyroxene is very close in composition to the primary low-Ca pyroxene in Divnoe (Fig. 17b),

TABLE 8. Compositions of model melts and residues (wt.%)

	1	2	3	4	5
SiO_2	58.96	54.75	59.29	37.60	34.97
TiO_2	0.27	0.32	0.55	0.03	0.02
Al_2O_3	3.93	10.22	16.49	0.73	0.68
FeO	16.30	13.56	6.53	16.17	15.04
MnO	0.27	0.29	0.14	0.44	0.41
MgO	8.32	8.26	1.76	33.06	30.75
CaO	9.59	7.99	6.07	1.63	1.52
Na_2O	1.38	4.26	8.29	0.16	0.15
K_2O	0.10	0.33	0.75	0	0
P_2O_5	0.89	0.05	0.12	0	0
Fe_{met}	-	-	-	10.19	9.48
Fe_{tot}	12.67	10.54	5.08	22.16	21.16
Total	100	100	100	100	93.01

1 - Melt in equilibrium with Divnoe residue
2 - Melt in equilibrium with model Acapulco residue
3 - Melt removed from Acapulco model source region
4 - All residual solids in model source region
5 - Col. 4 recalculated so the total equals to the sum of the same components in Divnoe; Table 5, col. 1

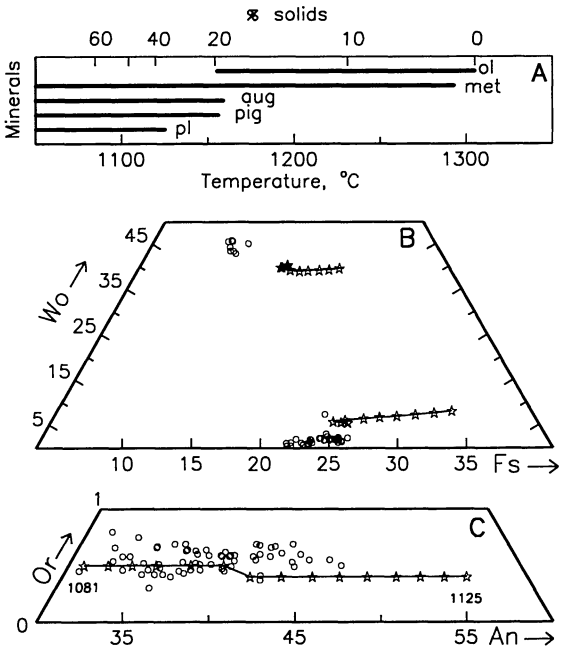

FIG. 17. Modelled crystallization of partial melt derived from an Acapulco source region. (a) the crystallization sequence; (b) pyroxene compositions; (c) plagioclase compositions. Ol - olivine, met - metal, aug - augite, pig - low-Ca pyroxene (pigeonite), pl - plagioclase. Circles, Divnoe minerals; stars, "model" minerals. While the crystallization sequence is in good agreement with petrographic observations, the expected pyroxenes are in general more ferrous than those in Divnoe. The first plagioclase crystallized is ~8 mol% more anorthitic than the cores of Divnoe plagioclases, but as temperature decreases the composition of the model plagioclase comes to match that of Divnoe plagioclase.

but it becomes more ferrous as temperature decreases. The augite has similar Wo content to that of Divnoe primary augite, but higher Fe contents. Plagioclase appears after 36% crystallization. The first plagioclase is ~8 mol% more anorthitic than the cores of Divnoe plagioclases (Fig. 17c), but as temperature decreases, the composition of the "model" plagioclase comes to match that of Divnoe plagioclase.

Since plagioclase is the only Divnoe mineral having pronounced igneous zoning, the compositions of its rims may record the cessation of partial melt crystallization, which probably resulted from a removal of Si, Al, Na, and K-rich melt (Table 8, column 3) from the source region after a ~60% degree of crystallization. The mineral assemblage left in the source region ("model Divnoe" composition) would consist of 77.6 wt% olivine, 9.9% metal, 3.2% low-Ca pyroxene, 2.1% high-Ca pyroxene, and 1.1% plagioclase (total 93.9%; 6.1% was removed with partial melt). This is very close to the Divnoe normative mineralogy (Table 6), except Divnoe has a higher low-Ca pyroxene content. However, the normative low-Ca pyroxene content of Divnoe represents both PP and ORL pyroxene combined, and the exact proportions of these are not known. In the model calculations, we did not consider ORL formation. If we assume a ~10 wt% content of ORL and subtract its pyroxene contribution (4–5%) from the normative low-Ca pyroxene content, the normative amount of PP low-Ca pyroxene approaches that of the "model Divnoe" composition. Also, reaction between the melt and residual olivine, which is consistent with petrographic observations, would slightly increase the model amount of low-Ca pyroxene. This reaction could also explain the depletion of orthopyroxene rims in Ca, Al and Cr, since these elements are highly depleted in olivine.

If equilibrium was maintained between the olivine residue and pyroxenes that crystallized from the melt, the olivine should become richer in Fe, and pyroxene should become poorer as a result of Fe-Mg exchange between them. The amount of Fe needed to increase Fa in model olivine to 25 mol% would be similar to the amount released by model pyroxenes if their Fs contents were reduced to the values found in Divnoe pyroxenes. It is interesting to note that the bulk composition of "model Divnoe" (Table 8, columns 4 and 5) is close to that of real Divnoe (Table 5), although the two do not match exactly.

High temperatures in the Divnoe source region should also result in melting of the metal-sulfide assemblage and fractionation of Ni, Fe, and S relative to one another. While the initial concentrations of these elements are not known, the initial Ni/Fe ratio can be safely assumed to be cosmic, and the amounts of Fe and S can be taken to be those observed in Divnoe.

The amount and composition of the melt can be estimated from the phase diagram of the Fe-Ni-S system (Chukhrov, 1974). At ~1300 °C (the estimated temperature in the final stages of partial melting in Divnoe source region, and assuming the relative abundances of Fe, Ni, and S mentioned above), ~31 wt% of these elements exist as melt (12.9 wt% Ni, 68.3% Fe, and 18.8% S) in equilibrium with mean Divnoe metal, containing 7.3 wt% Ni (Table 5). The rare occurrence of metal-troilite intergrowths in Divnoe, in contrast to the case in chondrites, indicates that most of the primary sulfide has been melted and separated from the primary metal. The presence of Ni-rich metal-sulfide inclusions in pyroxenes also implies the coexistence of silicate and Ni-rich metal-sulfide melts. The segregation of such a melt from unmelted residue should result in a ~36% depletion in Ni and complete removal of S from the residue.

The bulk analysis of Divnoe (Table 5) does show a ~39% depletion of the meteorite in Ni relative to cosmic Ni/Fe ratio but not in S. This suggests that another process has resulted in incorporation of S, which had become separated from Ni. The S in Divnoe is mainly concentrated in thin veinlets at grain boundaries and within ORL. Phase relations in the Fe-Ne-S system suggest that, at high temperatures, S has a high fugacity and could be separated from Ni and Fe as a gas and transported from the molten Fe, Ni and S-rich reservoir to the residue, where the S gas reacted with Fe. The presence of such a reservoir in the source region is indirectly indicated by large metal-sulfide veins in Divnoe containing fragments of different lithologies (Fig. 3). We will show below that transport of S in the gas phase, followed by its reaction with Fe^{2+} in olivine, has been a major factor in ORL formation.

Origin of the Divnoe Lithologies

Coarse-grained lithology–Our calculations indicate that material residual after partial melting in the Divnoe source region should consist of olivine and metal that was heated to ~1300 °C without melting, which is in good agreement with the structural characteristics and mineralogy of CGL. The composition of small metal-troilite inclusions in olivine also suggests that they have not experienced an igneous fractionation event in contrast to the inclusions in pyroxenes. Therefore, the host crystals of these inclusions have never been molten, and the structure of CGL was formed by high-temperature recrystallization of precursor material followed by its partial melting. The preferred alignment of elongated mineral grains in Divnoe suggests that partial melting might have taken place under stresses which caused some movement (by solid state flow?) of the Divnoe minerals within the source region.

Minor compositional differences between model and Divnoe olivine can be explained either by reaction between the melt and residue, or by subsolidus reequilibration of mafic silicates as is recorded by olivine-orthopyroxene thermometry. However, the range of variation of Fe content among olivine grains in both CGL and ORL (Fig. 6) is rather large, about twice as great as the fine-scale variations within the grains themselves. This suggests that the variations are primary in nature, and complete equilibrium (in the thermodynamic sense) was not attained in Divnoe during the partial melting of precursor material or during subsolidus cooling. It also implies that the precursor material was an unequilibrated chondrite.

One principal constituent of CGL, chromite, has not been taken into consideration in the model, but the morphologies of CGL chromites are consistent with their presence as primary minerals in the residue. It should be noted that some euhedral chromite grains found within PP could have crystallized from the melt.

Poikilitic patches–This lithology in Divnoe appears to represent volumes of partial melt that crystallized *in situ*. The textures of PP indicate that they formed during relatively slow crystallization from a melt enriched in normative pyroxene. The difference in composition between model and real pyroxenes is admittedly difficult to explain. While the difference in Fs contents could be explained either by reaction between melt and residue or by subsolidus reequilibration, the 2–2.5x higher concentrations of Al_2O_3 in model pyroxenes than those in Divnoe indicate a lower Al_2O_3 content of the melt that crystallized these pyroxenes. An

initially lower concentration of Al_2O_3 in the melt would also result in a minor decrease in the crystallization temperature of plagioclase and a lower An content, which would improve the agreement between model plagioclase compositions and those in Divnoe. Depletion of the partial melt in Al could result from either a nonchondritic composition of the Divnoe source region, or a removal of the earliest portions of partial melt enriched in most incompatible elements. The later suggestion is in a good agreement with the Divnoe source region composition estimated above and also with the REE patterns of Divnoe minerals (Davis *et al.*, 1993; A. M. Davis, pers. comm.), which appear to have crystallized from a LREE-depleted melt. Thus, minor and trace element abundance patterns in Divnoe minerals were probably established by partial melting in the source region and removal of the earliest fraction(s) of the partial melt, which were enriched in the most incompatible elements.

Plagioclase plays a special role in interpretation of the origin of Divnoe. Its textural position as a mineral filling spaces between mafic silicates, metal and chromite grains, and large metal-troilite veins (Fig. 5), suggests that it was the last silicate phase to crystallize from the melt, just before one or more powerful catastrophic event(s) resulted in the introduction of metal-sulfide melt into large cracks and the removal of uncrystallized residual melt. This could have been an impact, or an "explosive volcanic" process (Wilson and Keil, 1991).

Opaque-rich lithology–The origin of this lithology was the most controversial issue in the previous study of Divnoe (Zaslavskaya *et al.*, 1990). These authors assumed it was created by an energetic impact after the system solidified from its primary igneous event; the impact melted and mixed silicate and opaque minerals. However, this interpretation is inconsistent with the lack of shock features and melting in plagioclase grains that are in direct contact with ORL.

In the present study, we interpret the enrichment of ORL in opaque minerals, and the more magnesian composition of its silicates (relative to CGL and PP), as resulting from an extraction of Fe^{2+} from silicates to troilite. This could have been due to a reaction between gaseous sulfur and fayalite dissolved in the olivine of CGL,

$$Fe_2SiO_{4(s)} + MG_2SiO_{4(s)} + S_{2(g)} = 2FeS_{(s,l)} + Mg_2Si_2O_{6(s)} + O_{2(g)}$$

with the sulfur fugacity buffered by the troilite-metal assemblage in the source region. At the oxygen fugacity estimated for the Divnoe source region (IW-1.8) and assuming Divnoe silicate compositions (Tables 2 and 3), this reaction proceeds to the right at all temperatures.

Since ORL texture is indicative of an igneous origin, this could have occurred during the final stages of partial melting when all other solid minerals except olivine and metal were exhausted from the source region. In microchambers (tens to hundreds μm in size) represented now by ORL, reaction between olivine and gaseous sulfur resulted in extraction of Fe^{2+} from the silicate and the formation of troilite. This increased Si/(Fe + Mg) in the silicates of the microchamber, so the composition of the silicate portion of the microchamber became pyroxene-normative with the amount of pyroxene increasing as reaction proceeded. If the temperature in the microchamber was higher than its peritectic temperature, reaction between S and olivine resulted in an assemblage of molten troilite and pyroxene-rich silicate melt with as-yet-unreacted olivine. Since the temperature in the microchamber was fixed at any given time, the increase in Si/(Fe + Mg) resulted in an increase in the abundance of melt in the microchamber. At the same time, extraction of Fe from the silicates increased Mg/(Mg + Fe) in silicates in the microchamber and, therefore, the liquidus temperature of the silicates. Thus, if the temperature in the microchamber was fixed, melting soon would have stopped. If the temperature in the source region was rising, melting would have continued.

This idealized scheme can explain the texture and mineralogy of troilite-rich domains of ORL. However, the pyroxene formed in such a reaction should be ferromagnesian and contain only minor amounts of Mn. While the reaction produces pure enstatite, this exchanges Mg for Fe by reaction with olivine. The ORL pyroxene contains relatively small concentrations of minor elements other than Mn; therefore, some phase must have contributed these elements to the microchambers. Since the olivine residue in the source region coexisted with a partial melt, small amounts of the melt trapped at the olivine grain boundaries may have been this source phase. Close to the boundary between a small volume of melt and olivine, reaction between S and olivine would result in melting of the latter and growth of the volume of melt. The newly formed pyroxene-rich melt would supply the microchamber only with Si, Mg, Fe, and Mn; this would explain the depletion of ORL pyroxene in all minor elements except Mn as resulting from the dilution of earlier melt with ferromagnesian pyroxene. Since increasing the amount of melt decreases Fe/(Fe + Mg) in a microchamber, depletion of minor elements there (except Mn) must correlate negatively with this ratio. Only Mn, which is supplied to the melt from olivine, should display no depletion.

The temperature regime in the Divnoe source region also played an important role in producing ORL. While the temperature was rising, continuous melting could produce a major amount of ORL, which would drain away through pre-existing cracks and react with their walls. After temperature peaked, only small amounts of additional ORL could be formed, which remained in the residue. This means that ORL in Divnoe is the product of a predictable stage in the partial melting of its source region. It is the last portion of melt which formed, and it did not become segregated from the residue because it formed just as the source region began to cool. Minor variations in silicate compositions, even in small ORL domains, suggest that the partial melting in the Divnoe source region was not monotonic but episodic.

Some ORL domains are enriched in metal or associated with large CGL metal grains that show no evidence of ever having been molten. In such microchambers, the reaction between S and olivine produced silicate melt and liquid troilite, which reacted with metal to form metal-sulfide melt. The amount of such melt would have been even larger than that of pure-troilite melt.

During cooling of the Divnoe source region, ORL silicates should have crystallized much earlier than those of PP, which would explain the reaction boundary between ORL and CGL and the smooth boundary between ORL and PP. The sulfide or metal-sulfide melt in ORL crystallized later than the silicates, and it produced a more pronounced micrographic structure than the latter because the composition of the melt was closer to the eutectic composition.

Subsolidus Processes

The principal occurrence which disturbed the olivine-orthopyroxene equilibrium was a secondary heating event, which

raised the temperature of Divnoe by 100–200 °C for a short period of time. This was followed by rapid cooling, which suggests a shock event. The level of shock recorded in Divnoe silicates should have been accompanied by a local temperature increase of this magnitude (100–150 °C; Stöffler *et al.*, 1991). Moderate shock could also account for the reverse Cr zoning observed in olivine and orthopyroxene as well as ubiquitous troilite veins. Post-shock cooling was fast enough to freeze the compositions of pyroxene rims and the Cr content of olivine.

This shock event also should have formed Neumann bands and ϵ-structure in metal, and shock-induced twins in troilite (Stöffler *et al.*, 1988). The absence of these features in Divnoe metal and troilite points to a later low-temperature annealing that was sufficient to recrystallize metal and troilite but not silicates. This long low-temperature (80–200 °C) annealing is also required to explain the difference in distributions of cosmic-ray track lengths and densities between olivine and pyroxene (Petaev *et al.*, 1990c). The cosmic-ray exposure age of Divnoe (20 Ma) estimated from the measured track density is the same as that calculated from the noble gas data (O. Eugster; pers. comm.), implying that the required annealing might have taken place after breakup of the Divnoe parent body.

An unusual feature of Divnoe is the lamellar structure observed in most of its olivine grains. This is a real puzzle, since some particular process was required to produce fine-scale chemical zoning within the well-recrystallized rock. By transmitted light (Fig. 4a), the lamellae look very similar to deformation lamellae formed by stress in terrestrial mantle olivines (Deer *et al.*, 1982). The texture of Divnoe suggests that the same might be the case for Divnoe olivines, but this cannot explain the chemical differences between lamellae.

It is known from meteorites (Binns *et al.*, 1969; Smith and Mason, 1970; Steele and Smith, 1978; Putnis and Price, 1979; Price *et al.*, 1979) and experimental studies (Katsura and Ito, 1989; Akaogi *et al.*, 1989) that high-pressure transformations between $(Mg,Fe)_2SiO_4$ polymorphs could have produced chemical differences found in Divnoe olivines, but no high-pressure phases have been found in Divnoe to date. While exsolution has not been observed in ferromagnesian olivine solid solutions, the latter do have a calculated miscibility gap below 340 °C (Sack and Ghiorso, 1989). However, exsolution across this miscibility gap should have produced lamellae with even larger compositional difference than those found in Divnoe. Moreover, exsolution has not been found in pallasitic olivines, which cooled much slower than Divnoe olivines.

Another explanation for the olivine lamellae would be diffusion or deposition of Fe along tilt boundaries produced by shock deformation and annealing (H.Takeda; pers. comm.). However, this mechanism involves the reduction of Fe^{2+} in olivine to produce pyroxene, and neither reduced Ni-free Fe nor pyroxene have been found within lamellar olivine grains. The actual mechanism of formation of the lamellae might combine some of those discussed above, but clearly we do not have data enough to solve the puzzle. Further studies of the lamellar olivine are in progress; results will be reported elsewhere.

Divnoe and Other Meteorite Types

The oxygen isotope data clearly indicate a difference between Divnoe and all other meteorites. Only brachinites could be derived with Divnoe from a common oxygen reservoir, but the bulk and mineral chemistry of these two meteorite types militate against an origin in the same, homogeneous parent body.

Another group of meteorites whose possible affinity to Divnoe has been suggested is acapulcoites/lodranites (McCoy *et al.*, 1992). While these cannot have been derived from same parent body as Divnoe unless the object was isotopically inhomogeneous, the structural similarity between Divnoe, especially its CGL, and lodranites is impressive; their subsolidus cooling histories, including a secondary heating event followed by fast cooling (Miyamoto and Takeda, 1991), are also very similar. The substantial difference in oxidation state of Fe between the two types of meteorite need not be an obstacle to deriving the Divnoe composition (by the model discussed above) from an Acapulco-type source region through partial melting, crystallization, and removal of a portion of the partial melt.

What this indicates is that the parent bodies of Divnoe and acapulcoites/lodranites seem to have evolved similarly. Only the latest stages of igneous evolution of these meteorites seem to have been slightly different, judging by their different plagioclase compositions. Our thermodynamic calculations suggest that the depletion of Divnoe plagioclase in Na and K resulted from the removal of the partial melt from its source region at the final stages of crystallization. The nearly chondritic plagioclase composition of acapulcoites/lodranites suggests that a portion of their partial melt(s) was separated from the residue and transported locally within the source region, but was not removed from there. The enrichment of acapulcoites/lodranites in incompatible elements (Palme *et al.*, 1981) seems to support this suggestion.

CONCLUSION

Divnoe is a unique meteorite and the only known sample of its parent body. That body was chondritic in composition and very close in bulk chemistry to acapulcoites, except for a difference in Fe oxidation states and minor variations in other element abundances. The parent body evolved similarly to those of primitive achondrites. The Divnoe parent body experienced ~20% partial melting at ~1300 °C, after which a portion of partial melt (~60%) crystallized. The remaining liquid (~40%), which was rich in incompatible elements, was removed by a catastrophic event. This removal of partial melt depleted the Divnoe plagioclase in Na and K compared to other primitive achondrites. The mineral assemblages left in the source region are represented by olivine-rich CGL (the residue of original partial melting), plagioclase-pyroxene PP (partial melt that crystallized *in situ*), and troilite- and orthopyroxene-enriched ORL (produced by reaction between silicates and S vapor during partial melting). Thereafter, the parent body cooled slowly to ~500 °C, whereupon an impact event reheated it to ~700 °C for a short time. Later, probably after the parent body breakup, Divnoe experienced low-temperature (< 200 °C) annealing, which erased shock features from metal and troilite. At some stage of the subsolidus cooling, a poorly understood mechanism produced lamellar structure in the olivine grains.

Acknowledgements–We are very grateful to R. O. Sack for calculations of equilibrium temperatures; J. T. Wasson, G. W. Kallemeyn, and A. M. Davis for making their data available before publication; C. Robinson and B. B. Holmberg for assistance in microprobe analyses; and J. A. Wood and U. B. Marvin for invaluable help and discussions. Kind and constructive reviews by T. J. McCoy, M. Prinz, H. Takeda, and P. H. Warren greatly improved the manuscript and are appreciated. This work was supported by NASA Grants NAG9-28 to J. A. Wood and NAG9-48 to M. E. Lipschutz, and NSF grant EAR-92-18857 to R. N. Clayton. Support for neutron irradiations was provided by DOE under grant DE-FG07-80ER1 072 SJ.

Editorial handling: P. H. Warren

REFERENCES

AKAOGI M., ITO E. AND NAVROTSKY A. (1989) Olivine-modified spinel-spinel transitions in the system Mg_2SiO_4-Fe_2SiO_4: Calorimetric measurements, thermochemical calculation, and geophysical application. *J. Geophys. Res.*, **94**, B15671–B15685.

ANDERSON A. T., CLAYTON R. N. AND MAYEDA T. K. (1971) Oxygen isotope thermometry of mafic igneous rocks. *J.Geol.* **79**, 715–729.

ARISKIN A. A., BARMINA G. S. AND FRENKEL M. YA. (1991) Simulation of the crystallization of lunar-basalt melts. *Geochem. Int.* **28**, 92–100.

ARISKIN A. A., BORISOV A. A. AND BARMINA G. S. (1992) Simulating iron-melt equilibrium for silicate systems (abstract). *Lunar Planet. Sci.* **23**, 35–36.

BEZMEN N. I., LYUTOV V. S. AND OSADCHY E. G. (1978) Raspredelenie nikelya mezhdu troilitom i metallicheskim zhelezom kak mineralogicheskii termometr (Distribution of nickel between troilite and metal as a mineralogical thermometer). *Geokhimiya* **10**, 1466–1473.

BILD R. W. AND WASSON J. T. (1976) The Lodran meteorite and its relationship to the ureilites. *Mineral. Mag.* **40**, 721–735.

BINNS R. A., DAVIS R. J. AND REED S. J. B. (1969) Ringwoodite, natural $(Mg,Fe)_2SiO_4$ spinel in the Tenham meteorite. *Nature* **221**, 943–944.

BISWAS S., WALSH T. M., NGO H. T. AND LIPSCHUTZ M. E. (1981) Trace element contents of selected Antarctic meteorites–II. Comparison with non-Antarctic specimens. *Mem. Natl. Inst. Polar Res., Spec. Issue* **20**, 221–228.

BREARLEY A. J., RUBIE D. C. AND ITO E. (1992) Mechanisms of the transformations between α, β, and γ polymorphs of Mg_2SiO_4 at 15 GPa. *Phys. Chem. Minerals* **18**, 343–358

CHUKHROV F. V. (ED.) (1974) *Mineraly. Spravochnik. Diagrammy fazovykh ravnovesii (Minerals Handbook. Phase Diagrams. Issue 1).* Nauka, Moscow. 61pp.

CLAYTON R. N. (1993) Oxygen isotopes in meteorites. *Ann. Rev. Earth Planet. Sci.* **21**, 115–119.

CLAYTON R. N. AND MAYEDA T. K. (1992) Oxygen isotopic compositions of achondrites. *Proc. NIPR Symp. Antarc. Meteorites* **5**, in press.

DAVIS A. M., PRINZ M. AND WEISBERG M. K. (1993) Trace element distributions in primitive achondrites (abstract) *Lunar Planet. Sci.* **24**, 375–376.

DEER W. A., HOWIE R. A. AND ZUSSMAN J. (1982) *Rock-forming Minerals. Vol. 1A, Orthosilicates.* Longman, London. 919 pp.

D'YAKONOVA M. I., KHARITONOVA V. YA. AND YAVNEL' A. A. (1979) *Khimiya Meteoritov (Chemistry of Meteorites).* Nauka, Moscow. 68 pp.

FONAREV V. I. AND GRAPHCHIKOV A. A. (1991) Two-pyroxene thermometry: A critical evaluation. In *Progress in Metamorphic and Magmatic Petrology* (ed. L. L. Perchuk), pp. 65–92. Cambridge Univ. Press, Cambridge, U. K.

GRAHAM A. (ED.) (1983) The Meteoritical Bulletin, #61. *Meteoritics* **18**, 77–83.

JACKSON E. D. (1969) Chemical variation in coexisting chromite and olivine in chromite zones of the Stillwater complex. *Econ. Geology* **4**, 41–47.

JAROSEWICH E. (1990) Chemical analyses of meteorites: A compilation of stony and iron meteorite analyses. *Meteoritics* **25**, 323–337.

KATSURA T. AND ITO E. (1989) The system Mg_2SiO_4-Fe_2SiO_4 at high pressures and temperatures: Precise determination of stabilities of olivine, modified spinel and spinel. *J. Geophys. Res.* **94**, B15663–B15670.

KRING D. A. AND BOYNTON W. V. (1992) The trace element composition of Eagles Nest and its relationship to other ultramafic achondrites (abstract) *Lunar Planet. Sci.* **23**, 727–728.

KRINOV E. L. (1984) Morfologiya kamennykh meteoritov Preobrazhenka, Krutikha, Divnoe, Kamyshla (Morphology of the stony meteorites Preobrazhenka, Krutikha, Divnoe, Kamyshla). *Meteoritika* **43**, 19–25.

LINDSLEY D. H. AND ANDERSEN D. J. (1983) A two-pyroxene thermometer. *J. Geophys. Res.* **88**, Suppl. A887–A906.

MADON M. AND POIRIER J. P. (1983) Transmission electron microscope observations of α, β and γ $(Mg,Fe)_2SiO_4$ in shocked meteorites: Planar defects and polymorphic transitions. *Phys. Earth Planet. Inter.* **33**, 31–44.

MCCOY T. J., KEIL K., MAYEDA T. K. AND CLAYTON R. N. (1992) Petrogenesis of the Lodranite-Acapulcoite parent body (abstract). *Meteoritics* **27**, 258–259.

MIYAMOTO M. AND TAKEDA H. (1991) Cooling histories of primitive achondrites Yamato 74357 and MAC88177 (abstract). *Meteoritics* **26**, 374.

MUKHERJEE A. B., BULATOV V. AND KOTELNIKOV A. (1989) New high P-T experimental results on orthopyroxene-chrome spinel equilibrium and a revised orthopyroxene-spinel cosmothermometer (abstract). *Lunar Planet. Sci.* **19**, 731–732.

NAGAHARA H. AND OZAWA K. (1986) Petrology of Yamato-791493, "lodranite": melting, crystallization, cooling history, and relationship to other meteorites. *Mem. Natl.Inst. Polar Res., Spec. Issue* **41**, 181–205.

NEHRU C. E., PRINZ M., DELANEY J. S., DREIBUS G., PALME H., SPETTEL B. AND WÄNKE H. (1983) Brachina: A new type of meteorite, not a chassignite. *Proc. Lunar Planet. Sci. Conf.* **14th**, *J. Geophys. Res.* **88**, Suppl. B237–B244.

NEHRU C. E., PRINZ M., WEISBERG M. K., EBIHARA M. E., CLAYTON R. N. AND MAYEDA T. K. (1992) Brachinites: A new primitive achondrite group (abstract). *Meteoritics* **27**, 267.

PALME H., SCHULTZ L., SPETTEL B., WEBER H. W., WÄNKE H., CRISTOPHE MICHEL-LEVY M. AND LORIN J.C. (1981) The Acapulco meteorite: Chemistry, mineralogy and irradiation effects. *Geochim. Cosmochim. Acta* **45**, 727–752.

PETAEV M. I. AND ARISKIN A. A. (1992) Thermodynamic modelling of the origin of the Divnoe achondrite (abstract). *Lunar Planet. Sci.* **23**, 1059–1060.

PETAEV M. I. AND ZASLAVSKAYA N. I. (1990) The Divnoe meteorite. V. Classification, proposed genesis, relation with other meteorite types (abstract). *Lunar Planet. Sci.* **21**, 946–947.

PETAEV M. I., BARSUKOVA L. D. AND KONONKOVA N. N. (1990a) Meteorit Novosiborsk (The Novosibirsk meteorite). *Meteoritika 49*, 41–57.

PETAEV M. I., BARSUKOVA L. D., KOLESOV G. M. ND ZASLAVSKAYA N.I. (1990b) The Divnoe meteorite. III. Bulk chemistry (abstract). *Lunar Planet. Sci.* **21**, 948–949.

PETAEV M. I., USTINOV V. I., PERELYGIN V. P., AND SHUKOLYUKOV YU. A. (1990c) The Divnoe meteorite. IV. Oxygen isotope and track studies (abstract). *Lunar Planet. Sci.* **21**, 950–951.

PETAEV M. I., BARSUKOVA L. D., SHUMSKAYA T. V., ROMASHOVA T. V., GALUZINSKAYA A. K. AND SMOLIAR M. I. (1992) The Divnoe achondrite. VI. New data on bulk chemistry (abstract). *Lunar Planet. Sci.* **23**, 1061–1062.

PRICE G. D. (1983) The nature and significance of stacking faults in wadsleyite, natural β-$(Mg,Fe)_2SiO_4$ from the Peace River meteorite. *Phys. Earth Planet. Int.* **33**, 137–147.

PRICE G. D., PUTNIS A. AND AGRELL O. (1979) Electron petrography of shock-produced veins in the Tenham chondrite. *Contrib. Miner. Petrol.* **71**, 211–218.

PRICE G. D., PUTNIS A. AND SMITH D. G. W. (1982) A spinel to β-phase transformation mechanism in $(Mg,Fe)_2SiO_4$. *Nature* **296**, 729–731.

PUTNIS A. AND PRICE G. D. (1979) High pressure $(Mg,Fe)_2SiO_4$ phases in the Tenham chondritic meteorite. *Nature* **280**, 217–218.

SACK R. O. AND GHIORSO M. S. (1989) Importance of considerations of mixing properties in establishing an internally consistent thermodynamic database: Thermochemistry of minerals in the system Mg_2SiO_4-Fe_2SiO_4-SiO_2. *Contrib. Miner. Petrol.* **102**, 41–68.

SACK R. O. AND GHIORSO M. S. (1991) Chromian spinels as petrogenetic indicators: Thermodynamics and petrological applications. *Am. Mineral.* **76**, 827–847.

SMITH J. V. AND MASON B. (1970) Pyroxene-garnet transformation in the Coorara meteorite. *Science* **168**, 832–833.

SMOLIAR M. I., PETAEV M. I. AND SHUKOLYUKOV YU. A. (1991) Divnoe meteorite: Preliminary results of Rb-Sr age dating (abstract). *Lunar Planet. Sci.* **22**, 1281–1282.

STEELE I. M. AND SMITH J. V. (1978) Coorara and Coolamon meteorites: Ringwoodite and mineralogical differences (abstract). *Lunar Planet. Sci.* **9**, 1101–1103.

STÖFFLER D., OSTERTAG R., JAMMES C., PFANNSCHMIDT G., SEN GUPTA P. R., SIMON S. B., PAPIKE J. J. AND BEAUCHAMP R. H. (1986) Shock metamorphism and petrography of the Shergotty achondrite. *Geochim. Cosmochim. Acta* **50**, 889–903.

STÖFFLER D., BISCHOFF A., BUCHWALD V. AND RUBIN A. E. (1988) Shock effects in meteorites. In *Meteorites and the Early Solar System* (eds. J. F. Kerridge and M. S. Matthews), pp. 165–202. Univ. Arizona Press,